LUMINESCENT PROBES OF HYDROPHOBIC SILICA AEROGELS

By

Christopher J. Backlund

****

Submitted in partial fulfillment
of the requirements for
Honors in the Department of Chemistry

UNION COLLEGE

June, 2009

Abstract

BACKLUND, CHRISTOPHER J. Luminescent Probes of Hydrophobic Silica Aerogels. Union College. Department of Chemistry, June 2009.

Aerogels have many applications such as platforms for sensing chemical species as well as insulation between windows. When Silica aerogels are exposed to water their nanostructure deteriorates. However, we can fabricate hydrophobic aerogels using Union's patented rapid supercritical extraction (RSCE) technique, in a hydraulic hot press. Varying degrees of hydrophobic aerogels have been fabricated using different mixtures of tetramethoxysilane (TMOS) and methyltrimethoxysilane (MTMS) via a base-catalyzed reaction. Sessile drop tests reveal that water beads on these hydrophobic aerogels with a contact angle of above 150 degrees. But does this surface hydrophobicity render the porous nanostructure impermeable to water? We describe here a series of spectroscopic experiments in order to ascertain the extent to which water vapor penetrates hydrophobic aerogels of varying degrees of hydrophobicity. We have entrapped and detected Rhodamine 6G, Fluorescein, and Rhodamine B in hydrophilic and hydrophobic aerogels to be used as humidity-sensitive probes. We have shown that the fluorescence emission signal of Fluorescein increases in response to increasing relative humidity. We have shown that hydrophobic aerogels are not impervious to water vapor. A humidity apparatus has been set up that will allow us to quantify the relative humidity of the aerogel environment while collecting fluorescence spectra. We describe here our spectroscopic evaluation of humidity-sensitive probes immobilized within hydrophobic and hydrophilic silica aerogels that are exposed to varying amounts of water vapor.

Acknowledgements:

I would first like to thank the Union College Chemistry Department and its faculty for giving me an excellent education and the opportunity to conduct this research. I would also like to thank my thesis advisor Professor Mary Carroll for all of her attention, guidance, and support throughout this project.

I would further like to thank the National Science Foundation for the funding they provided for the aerogel team (CTS-0216153 RUI/MRI, CHE-0514527 RUI, and MRI/CMMI-0722842). A thank you must also go out to the Union College Internal Education Fund and the Surdna Summer Fellowship for supporting my research.

A special thank you goes out to Professor Brad Bruno for his assistance with the camera set up and operation for measuring water droplet contact angles. I would also like to thank Emily Green for her past work in the lab that fostered this project. I also need to thank Stan Gorski for his help in fabricating part of the humidity apparatus used in this research.

Lastly, I would like to thank Kathy Ryan for her help throughout the course of the research, the aerogel team for their constant help and support, as well as all of my fellow chemistry majors for their support.

Table of Contents

Abstract i
Acknowledgements ii
Table of Figures iv
Table of Tables vi

Chapter 1: Introduction 1
Silica Aerogels 1
Drying Options 3
Hydrophobic Silica Aerogels 5
Hydrophobic Aerogels and Water Vapor 7
Luminescence Detection and Analysis 10
Humidity-Sensitive Luminescent Molecular Probes 12
Other Ways to Detect Humidity 15
Humidity Apparatus 16

Chapter 2: Experimental 18
Fabrication of Doped Sol-Gels 18
Fabrication of Hydrophobic Doped Sol-Gels 20
Rapid Supercritical Extraction 21
Analysis of Aerogels 24

Chapter 3: Results 28
Rhodamine B Humidity Tests 28
Rhodamine 6G Humidity Tests 30
Fluorescein Humidity Tests 34
Fluorescein Photobleaching 38
Fluorescein Humidity Tests Continued 38
Humidity Apparatus 42
Sessile Water Droplet Contact Angles 47

Chapter 4: Discussion 50
Rhodamine B 50
Rhodamine 6G 51
Fluorescein 52
Fluorescein Breakthrough 55
Humidity Apparatus 57
Sessile Water Droplet Contact Angles 59
Future Work 60

References 62

Table of Figures

Figure 1.	Schematic of polymerization reaction in TMOS aerogels	2
Figure 2.	Schematic of hot press set up in lab	4
Figure 3.	Structure of MTMS, a TMOS derivative	9
Figure 4.	Representation of a Jablonski diagram	11
Figure 5.	Structure of Rhodamine 6G	13
Figure 6.	Structure of Rhodamine Fluorescein	13
Figure 7.	Structure of Rhodamine B	14
Figure 8.	Photo of 16-well cuvette mold used to fabricate aerogels	22
Figure 9.	Schematic of humidity apparatus	27
Figure 10.	Fluorescence emission spectra 3.5 x 10^{-5} M RB (100% TMOS) aerogel from Tristar to room humidity	28
Figure 11.	Plot of signal versus time for 3.5 x 10^{-5} M RB (100% TMOS) aerogel from Tristar to room humidity	29
Figure 12.	Fluorescence emission spectra 10^{-4} M R6G (100%TMOS) aerogel from dessicator to room humidity	30
Figure 13.	Plot of signal versus time for 10^{-4} M R6G (100% TMOS) aerogel from dessicator to room humidity	31
Figure 14.	Fluorescence emission spectra 10^{-5} M R6G (50%TMOS/50%MTMS) aerogel from dessicator to room humidity	33
Figure 15.	Plot of signal versus time for 10^{-5} M R6G (50%TMOS/50%MTMS) aerogel from dessicator to room humidity	34
Figure 16.	Fluorescence emission spectra 5 x 10^{-4} M Fluorescein (100%TMOS) aerogel from dessicator to room humidity	35
Figure 17.	Plot of signal versus time for 5 x 10^{-4} M Fluorescein (100%TMOS) aerogel from dessicator to room humidity	36
Figure 18.	Fluorescence emission spectra 5 x 10^{-4} M Fluorescein (100%TMOS) aerogel from Tristar to room humidity	39

Figure 19. Plot of signal versus time for 5 x 10^{-4} M Fluorescein (100%TMOS) aerogel from Tristar to room humidity 40

Figure 20. Plot of signal versus time for 5 x 10^{-4} M Fluorescein (50%TMOS/50%MTMS) aerogel from Tristar to room humidity 41

Figure 21. Plot of signal versus time for 5 x 10^{-4} M Fluorescein (75%TMOS/25%MTMS) aerogel from Tristar to room humidity 41

Figure 22. Fluorescence emission spectra of 10^{-5} M R6G (100%TMOS) aerogel in the humidity apparatus 43

Figure 23. Fluorescence emission spectra of 10^{-5} M R6G (100%TMOS) aerogel in the humidity apparatus (N_2 gas test) 44

Figure 24. Fluorescence emission spectra of 10^{-5} M R6G (100%TMOS) aerogel in the humidity apparatus (repeat N_2 gas test) 45

Figure 25. Time based emission scan of (100% TMOS) 5 x 10^{-4} M Fluorescein aerogel while varying humidity 46

Figure 26. Image of sample sessile water droplet contact angle measurement 47

Table of Tables

Table 1.	Standard recipe used to fabricate standard sol-gels	18
Table 2.	Altered recipe to afford hydrophobic sol-gels	20
Table 3.	Process parameters for fabrication of aerogels in hot press	23
Table 4.	Humidity test responses for 100% TMOS R6G aerogels	32
Table 5.	Humidity test response for 5×10^{-4} M Fluorescein aerogels	37
Table 6.	Tristar humidity test response for 5×10^{-4} M Fluorescein aerogels	37
Table 7.	Photobleaching for 5×10^{-4} M Fluorescein aerogels	38
Table 8.	Tristar Humidity test 5×10^{-4} M Fluorescein aerogels	42
Table 9.	Measured sessile contact angles (pre formatting)	48
Table 10.	Measured sessile contact angles (post formatting)	49

Chapter 1: Introduction

Silica Aerogels

Silica aerogels can be synthesized via polymerization of tetramethylorthosilicate (TMOS) to form a solid, translucent silica backbone. These silica aerogels have an extensive nanoporous structure consisting of 90-99% air by volume giving them the lowest known density of any solid. Densities for silica aerogels have been observed below 0.25 g/cm^3.[1] Due to their high porosity, on the order of nanometer-sized pores, aerogels can have inner surface areas exceeding 1000 m^2/g.[1] The nanoscale pores also allow these materials to have the lowest known thermal, electrical, and acoustical conductivities of any known solid. The longitudinal acoustic velocity of aerogels is typically on the order of 100 m/s.[1] The solid thermal conductivity of a typical aerogel with density of 120 kg/m^3 is on the order of 5 mW/mK and the gaseous thermal conductivity does not exceed 10 mW/mK.[1] The translucent nature gives aerogels the lowest known index of refraction of any known solid and has been observed to be around 1.[1] With regard to the translucent nature of silica aerogels, an optical transmittance of up to 93% has been observed at a wavelength of 900 nm.[1]

The physical properties of silica aerogels make them incredibly useful for many applications. Aerogels have already been experimentally incorporated into boots and jackets for use as thermal insulators due to their low thermal conductivity.[2] The Navy is investigating the use of aerogels in undergarments for divers[3] and NASA is looking into them for incorporation into space suits for their

thermal insulation properties.[2] Cooling and heating systems, including hot and cold pipes, for hot or cold storage can be insulated using aerogels, as well.[1] Aerogels have in addition been incorporated between windowpanes for both their thermal insulation and translucent properties.[4] They have even been utilized in the insulation of the electronics used aboard the Sojourner Mars Rover.[1] Aerogels have furthermore been utilized for their acoustic insulation properties. As acoustic insulation, they have been investigated for use in floors of a home to reduce footfall noise and have also been applied to anechoic chambers.[1] Aerogels are of great interest for acoustic insulation of transportation and machinery, too.[5]

A standard reaction used to fabricate silica aerogels is the polymerization of tetramethyl orthosilicate (TMOS) with water in the presence of ammonium hydroxide as the catalyst and methanol as the solvent. In the Aerogel Lab at Union, these compounds are typically mixed together in a TMOS : methanol : water : ammonium hydroxide molar ratio of 1 : 12 : 4 : 3.7×10^{-3}. A schematic of the reaction can be seen below in Figure 1.

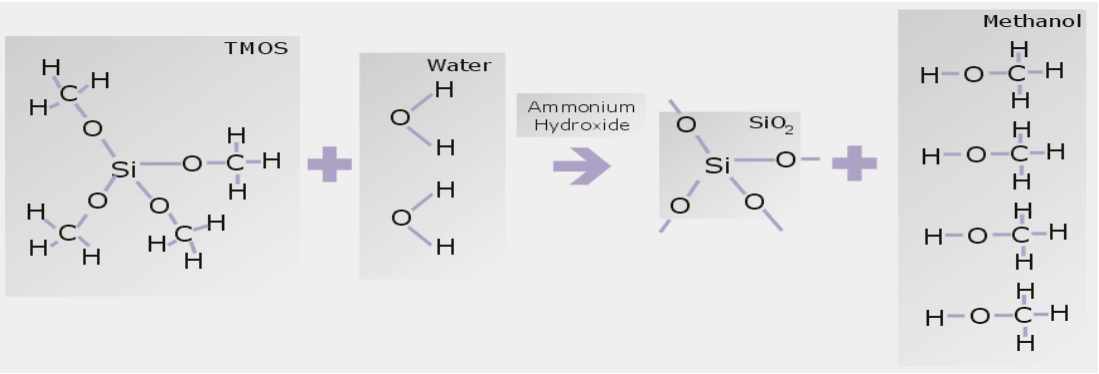

Figure 1: Schematic of polymerization reaction involved in fabricating TMOS based silica aerogels.[6]

This reaction affords what is known as a wet sol gel. A wet sol gel consists of the solid polymerized silica backbone with solvent, predominantly methanol, surrounding it. In order to obtain an aerogel, the solvent must be removed from the pores of the gel. This presents somewhat of a challenge because if the sol gel is allowed to dry under normal conditions, the surface tension from the methanol will be too great a force for the pores and the nanostructure of the sol gel will collapse; a xerogel, instead of an aerogel, will be produced. To create an aerogel, the methanol must be removed while maintaining the composition of the porous structure inside the gel.

Drying Options

In order to maintain the integrity of the nanostructure, two primary methods are employed. The first technique is the use of surfactants in the drying process and the second technique is accomplished through what is known as supercritical extraction of the solvent. The surfactant method consists of letting the wet sol gel dry under ambient conditions but using surfactants on the walls of the nanopores in order to relieve the surface tension produced by the receding methanol. The surfactant acts as a coating that prevents the methanol from directly coming in contact with the silica backbone, thereby reducing the tension of the receding methanol on the pore wall as it evaporates out of the sol gel.

The second option is supercritical extraction. This method involves solvent exchange washes to replace the methanol with some other solvent, typically CO_2, which can then be supercritically extracted from the sol-gel matrix.

To be supercritically extracted means to increase the temperature and pressure above the critical point of the solvent, causing the solvent to be neither liquid nor vapor, and then releasing pressure to allow the supercritical solvent to escape while maintaining an elevated temperature. Having the solvent be neither liquid nor vapor allows the solvent to escape without the presence of surface tension, allowing the porous nanostructure to remain intact. The supercritical extraction is usually done in an autoclave and it can take up to two weeks to form aerogel monoliths.

Here at Union College, we employ a patented[7] Rapid Supercritical Extraction (RSCE) technique, using a hydraulic hot press, which takes only a few hours to complete. This process involves loading the precursor solution (methanol, water, TMOS, and ammonium hydroxide) into a mold, which is then sealed by the hot press platens with kapton and graphite as the gasket material. A schematic of the mold and hot press set-up can be seen below in Figure 2.

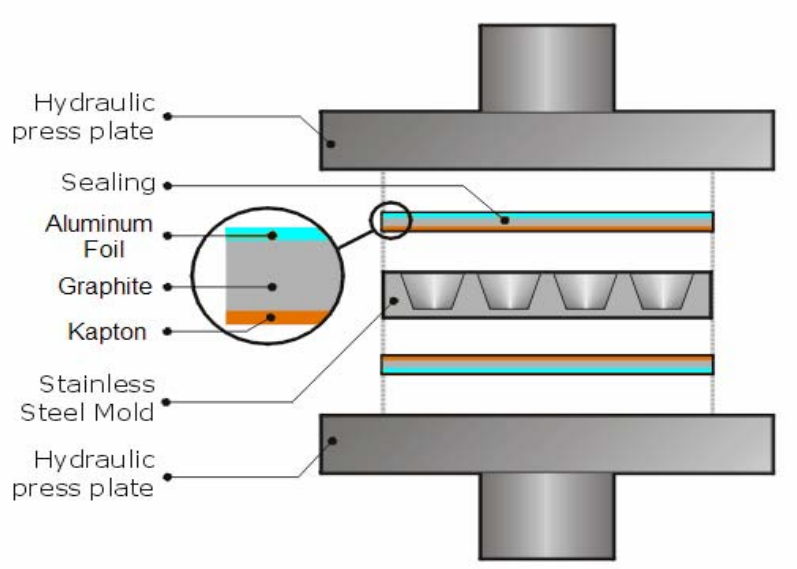

Figure 2: Schematic of mold and hot press set-up to fabricate aerogels using Union's Rapid Supercritical Extraction (RSCE) technique.[8]

The precursor material then gels in the mold within the hot press to afford a wet sol gel. The hot press subsequently takes the methanol supercritical by increasing temperature and pressure. When the methanol is above its supercritical point, the pressure applied by the hot press platens is released to allow the methanol to escape from both the wet sol gel and the mold. The temperature is afterward lowered to cool the resulting aerogel, leaving its extensive nanoporous structure still intact.

Hydrophobic Silica Aerogels

Silica aerogels comprised of TMOS are inherently hydrophilic solids. This is due to the properties of the TMOS compound that are being incorporated into the backbone of the aerogel as well as the nature of the reactions that are taking place during fabrication. The hydrolysis reaction on the TMOS produces hydroxyl groups that are utilized in the polymerization of the silica matrix backbone. This polymerization reaction will not use up all of the hydroxyl groups and some will be “left over” as free hydroxyl groups once the polymerization reaction is complete. The left-over hydroxyl groups on the silica backbone contribute to the overall hydrophilic properties of the material. Furthermore, the hydrolysis reaction of the TMOS is not completely successful and will fail to convert all the methoxy groups attached to the silica into hydroxyl groups. These “left over” methoxy groups are inherently polar in nature and can interact with water once hydrolysis has occurred. The polar methoxy groups on the silica, as well as the hydroxyl groups left over after the polymerization reaction, are

responsible for the inherently hydrophilic nature of aerogels fabricated with the compound TMOS. By altering the composition of the aerogel backbone, hydrophobic aerogels could be fabricated.

Methyltrimethoxysilane differs from TMOS in that it has only three methoxy groups bound to the central silica with the fourth branch being a methyl group. This molecule has been shown by others to produce hydrophobic aerogels when incorporated in a precursor solution with TMOS[9,10] and when subsequent supercritical drying occurred. These gels were shown to be hydrophobic by measuring the sessile contact angle of a drop of water on the surface of the gel as well as by measuring the uptake of water in a moist environment. It was also shown that alteration of the molar ratios in the precursor solution could affect the degree of hydrophobicity of the aerogel.[9,10] That is, the more hydrophobic precursor you use in place of TMOS, the more hydrophobic in nature the final aerogel becomes. Schwertfeger et al. noted that a similar solvent exchange method, utilizing supercritical extraction of CO_2, could not produce aerogels of comparable hydrophobicity when matched up to the supercritical extraction of methanol, but the reasoning behind this claim was not discussed.[10]

Hydrophobic TMOS-based silica aerogels prepared using methyltrimethoxysilane (MTMS), ethyltrimethoxysilane (ETMS), or propyltrimethoxysilane (PTMS) in the precursor solution have been fabricated by Emily Green using Union's RSCE method and the hydraulic hot press.[11] These aerogels were shown to be hydrophobic by measuring the sessile drop contact angle on the surface of the gel. A small droplet of water was placed on the

surface of the aerogel and the angle the drop made with the surface was measured using a camera and image software. Green demonstrated that when the percent of hydrophobic precursor is increased, the contact angle becomes greater, and it is therefore possible to produce aerogels of varying degrees of surface hydrophobicity. The varying degrees of hydrophobicity are characterized based on a % by volume system where the volume of TMOS used in the recipe was replaced with a mixture of TMOS and a TMOS derivative (MTMS, PTMS, ETMS). This percentage of derivative added to the recipe was denoted the % derivative for that aerogel (neglecting the volume contributions of the other components of the sol-gel precursor solution). For example, if the total amount of TMOS required was 20 mL and 10 mL of it was replaced with MTMS, the resulting aerogel would be classified as a 50% MTMS gel by volume. Several volume/volume mixtures were employed to create aerogels of varying hydrophobicity. The most hydrophobic aerogels with each precursor used 75% MTMS by volume and 50% for the PTMS and ETMS. The contact angles ranged from 95˚ for the hydrophilic TMOS aerogels to over 150˚ for each of the hydrophobic aerogels.[11]

Hydrophobic Aerogels and Water Vapor

With these studies complete, we have a good understanding of the hydrophobicity that can be attained at the surface of the aerogel. We know that water beads up on the surface of these hydrophobic aerogels and that it is possible to increase the degree of hydrophobicity at the surface level. This raises the

question: how hydrophobic are these aerogels when it comes to water vapor? Are these hydrophobic aerogels effective at repelling water vapor and does the hydrophobicity of the aerogel's surface completely prevent the permeation of water vapor into the gel? Does the degree of hydrophobicity of the aerogel have an influence on the degree of water vapor permeation through the aerogel? This is a crucial question to ask because a hydrophobic aerogel that is used as a barrier to water is useless if it allows water vapor to pass through. In the case of the window application, you don't want water getting through the aerogel onto the other side because it can reach your house. It could cause damage to the house and windows if water vapor is getting in and condensing inside these structures. The research presented in this thesis deals with this issue.

The extent to which water vapor permeates hydrophilic aerogels, as well as aerogels of varying degrees of hydrophobicity, is the topic of this thesis research. In order to investigate this issue, the TMOS backbone of the aerogels was organically modified using a TMOS derivative successfully used by former students in the group. Methyltrimethoxysilane (MTMS) had previously been used to successfully fabricate 0%, 25%, 50%, and 75% hydrophobic aerogels. This percent MTMS is again describing the percent by volume that the derivative is being added in place of the volume of TMOS called for in the "standard" recipe. For example, the 50% MTMS aerogel will have half the standard volume of TMOS and the rest of the volume would be derivative. The other derivatives used, ethylmethoxysilane (ETMS) and propylmethoxysilane (PTMS), were only used to fabricate 0%, 25%, and 50% derivative aerogels.[7] Furthermore, the

MTMS, ETMS, and PTMS-based aerogels had comparable contact angles of about 150˚ at 25% and 160˚ at 50% hydrophobicity.[11] The fact that a wider range of MTMS hydrophobic aerogels had been fabricated in the past, as well as the similar contact angles between the MTMS and the other compounds, led to MTMS being chosen as the derivative to modify the backbone of the silica aerogel for the work described in this thesis. The structure of MTMS can be seen below in Figure 3. Take note of the single methyl side chain that makes this compound more hydrophobic than TMOS.

MTMS

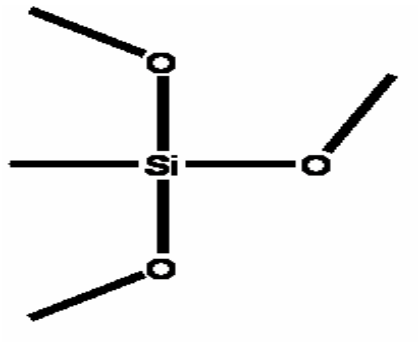

Figure 3: Structure of methyltrimethoxysilane (MTMS), a TMOS derivative used to organically modify the sol-gel backbone and create hydrophobic silica aerogels of varying degrees of hydrophobicity.

Silica aerogels were fabricated using various amounts of TMOS and MTMS as precursors. The recipes were altered so that TMOS was replaced by more and more MTMS, thereby increasing the hydrophobicity of the aerogels. The first task was to show that the fabricated aerogels were indeed hydrophobic. This was established by measuring the sessile water drop contact angle on the surface of the aerogel. The next step was to test the aerogel monoliths for their

resistance to water vapor permeation and compare the results to that for the hydrophilic ('standard') aerogel. This investigation of water vapor permeation through the aerogels was carried out via fluorescence emission spectroscopy.

Luminescence Detection and Analysis

Fluorescence, as defined by Harris[12], is the emission of a photon during a transition between states with the same spin quantum numbers. A molecule absorbs an incoming photon and the added energy promotes the molecule from the ground electronic state to an excited electronic state. From this excited state, the molecule can release its excess energy through a number of ways. The molecule can relax down to the ground electronic state through a nonradiative, vibrational relaxation, or it could either fluoresce or phosphoresce. If the molecule remains in a singlet state, which is common, the molecule can release its energy as a photon in the form of fluorescence and return to the ground-state energy level. If the molecule enters a triplet state from the lowest excited energy state the molecule can release a photon through phosphorescence in order to reach the ground state again. Phosphorescence is rare, occurs at lower energies than fluorescence and is usually observed when the molecule is cold or entrapped in a rigid environment. A schematic of the radiative processes fluorescence and phosphorescence can be seen below in Figure 4, in what is known as a Jablonski diagram.

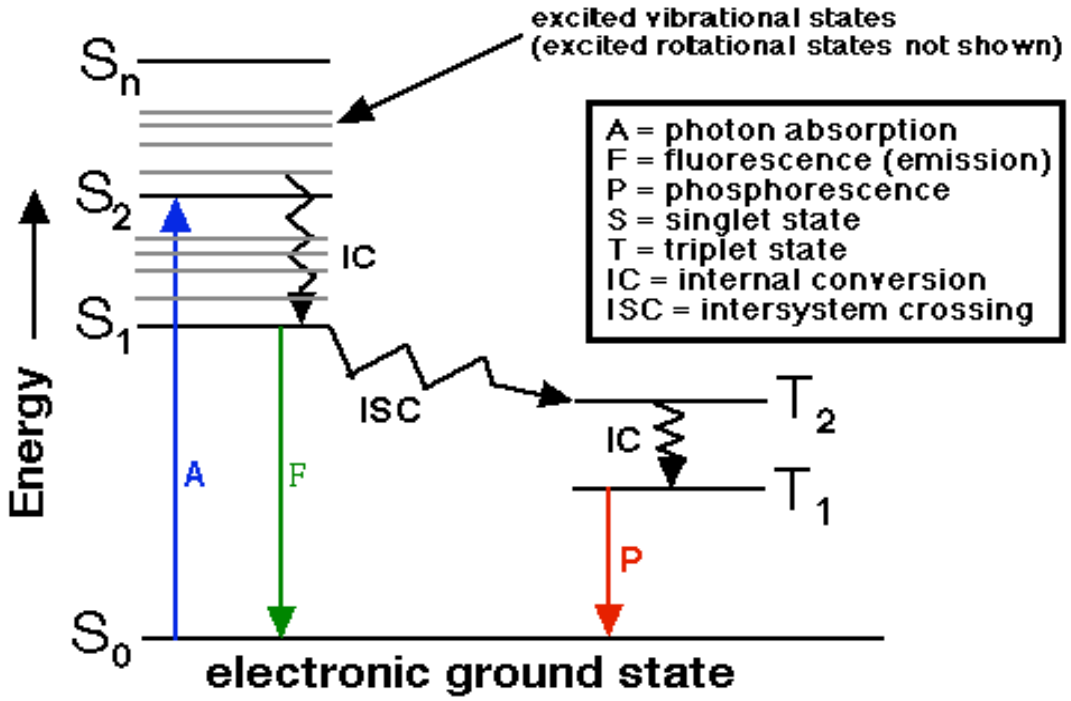

Figure 4: Jablonski diagram of the radiative processes of fluorescence and phosphorescence.[13]

In fluorescence, the molecule gives off light with energy equal to the energy difference between the lowest singlet excited energy state and the singlet ground state of the molecule. The photons given off from the molecule can then be detected in the lab using a fluorometer and the intensity of the emitted light can then be determined. The more photons that are absorbed by the molecule, the more photons are given off, so the intensity of the fluorescence will increase. The detection of the fluorescence emission intensity is the basis for the luminescent investigation of the hydrophobic aerogels.

Here at Union College, it has been shown[14] that the luminescent probe platinum(II) octaethylporphyrin (PtOEP) can be incorporated into the silica matrix of an aerogel during the RSCE technique and detected via luminescence

emission. It has also been shown that the PtOEP complex, entrapped in the aerogel, will luminesce differently when the environment of the aerogel is altered. PtOEP, entrapped in aerogels, has been shown to have great luminescence emission intensity in the presence of nitrogen gas but in the presence of oxygen, the fluorescence emission is quenched.[15] This probe, when entrapped in an aerogel, has an application to be an oxygen sensor as the emission will disappear when the aerogel is in the presence of oxygen. The important point here is that the emission intensity of the immobilized probe changes in response to the presence of oxygen, which is an environmental condition that can be controlled. This alteration of emission intensity due to the atmosphere surrounding the aerogel is the general idea behind using immobilized molecular probes, and their subsequent fluorescence emission, to determine the extent to which water vapor permeates through aerogels.

Humidity-Sensitive Luminescent Molecular Probes

For the research presented, luminescent probes for which the fluorescence emission intensity would change in response to varying levels of environmental humidity were sought. Three possible compounds were investigated. The first compound was Rhodamine 6G, a compound that fluoresces and has been shown by others to have an emission intensity response to changes in relative humidity.[16] According to previous research, the fluorescence emission intensity of this compound should decrease with an increase in relative environmental humidity.[17] This molecule was therefore selected as a viable candidate for monitoring

humidity changes. The structure of this fluorescent molecular probe can be seen in Figure 5, below.

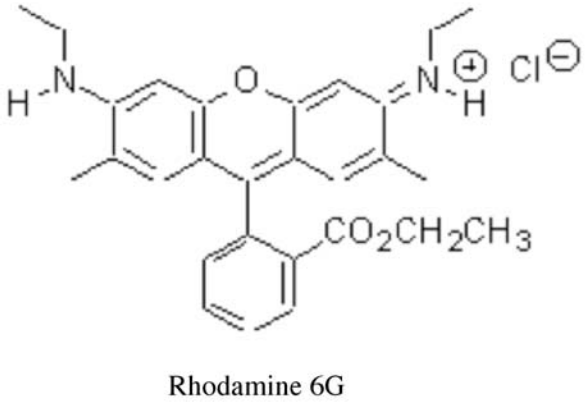

Figure 5: Structure of Rhodamine 6G.

A second compound with a reported fluorescence emission intensity response to different levels of relative humidity was Fluorescein.[16] The reported response of Fluorescein was unknown according to past research but we decided that it would become apparent as the molecule was tested. This was also chosen as a viable candidate for monitoring relative humidity changes within the aerogel. The structure of this fluorescent molecular probe can be seen below in Figure 6.

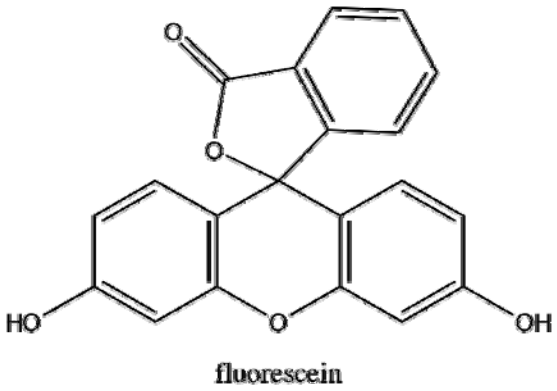

Figure 6: Structure of Fluorescein.

The third compound chosen was Rhodamine B. This compound has been reported to have a change in absorbance in response to environmental relative humidity.[18] More specifically, as the relative humidity increases, there is a reported large increase in absorbance in the visible region.[18] This increase in absorbance with increasing relative humidity should produce an increase in fluorescence emission with an increase in relative humidity. The structure of this compound can be seen below in Figure 7.

Figure 7: Structure of Rhodamine B.

The other factor that led to these three molecules being singled out for use in this research is that these three molecular probes have been successfully incorporated into aerogels using the RSCE technique and have been detected inside the aerogel via fluorescence emission intensity data here at Union College.[19,20] There is a concern when using the RSCE method that certain molecular probes lack the thermal stability required to survive the heat and pressure and will, therefore, not be detectable by fluorescence afterwards. But

since these probes were previously shown to survive and fluoresce, they were solid candidates for use as humidity sensors in aerogels prepared via the RSCE process. The process by which these aerogels were fabricated in the new hot press was modified from the original process used on a different hot press by previous researchers. Furthermore, the process was also combined with the process for fabricating hydrophobic aerogels in order to create new processes for creating hydrophobic and hydrophilic aerogels doped with Rhodamine 6G, Fluorescein, and Rhodamine B.

Other Ways to Detect Humidity

There are other ways in which humidity can be detected besides using fluorescent probes and obtaining steady-state emission scans. The use of cellulose impregnated with cobalt chloride in order to obtain quantitative relative humidity measurements was investigated by Boltinghouse and Abel.[21] They found that the sorption of water caused the structure to swell and that this altered the absorbance of the cobalt chloride. They showed that as the relative humidity increased, the absorbance of the $CoCl_2$ decreased.[21]

It is also common to have humidity sensors be based on water causing a change in the conduction properties of a substance. Zhu et al. showed that a pentacene thin-film transistor can be used to monitor humidity.[22] They noted that as the transistor was subjected to more and more humidity, the saturation current of the pentacene film decreased and that sensitivity was based on the thickness of the film.[22] Wang et al. showed that TiO_2 nanowires could also be synthesized for

use as humidity sensors.[23] They demonstrated that as the relative humidity experienced by the wires increased from 5% to 95%, there was a one and half order of magnitude decrease in the resistance of the wires.[23]

None of these methods were employed in this project, however. Fluorescence detection of humidity-sensitive molecular probes was the only method utilized.

Humidity Apparatus

A major issue that needed to be addressed in the design of the experiments was how to control and quantify the humidity inside the fluorescence cell containing the aerogel. In order to keep the humidity constant as well as to be able to quantify the humidity of the environment in which the aerogel was present, a humidity generator was needed. Takahashi and Kitano described the use of flow humidity generators in generating an atmosphere with a constant humidity.[24] Divided flow humidity generators involve dry air being split into two lines, one that remains dry and one that gets wet. The two branches then reunite, with different flows, producing varying degrees of relative humidity, and enter into the test chamber to produce the constant, desired humidity in the environment of interest. It was this design that spawned the creation of a prototype humidity apparatus that allowed for us to control the flow of humidity into the test chamber. This prototype also allowed us to quantify the relative humidity within the test chamber while still being able to quantify the fluorescence emission intensity of the probe in order to track the extent of water vapor permeation into

the aerogel. This allowed for the quantification of relative humidity, as well as subsequent water vapor permeation into the aerogel, at the same time.

Chapter 2: Experimental

Fabrication of Doped Sol-Gels

The precursor recipes used for the fabrication of the sol-gels in this research were adapted from the recipe given below in Table 1. This recipe is referred to as the "standard 40-mL recipe" as it has a total volume of 40 mL and is used to fabricate standard sol-gels.

Table 1: Standard recipe used to fabricate standard sol-gels

Precursor	Volume (mL)
Tetramethyl orthosilicate (TMOS)	8.50
Methanol (MeOH)	27.5
Deionized Water	3.60
1.5 M Ammonium Hydroxide	0.135

This recipe was utilized as the precursor for standard aerogels and xerogels. These components were combined in the lab and mixed for ten minutes via manual stirring with a disposable glass pasteur pipette before further processing. It should be noted that the amount of ammonium hydroxide catalyst used in for the aerogel fabrication described in this thesis was double the amount called for by the standard 40-mL recipe (Table 1). That is, 0.270 mL of 1.5-M ammonium hydroxide catalyst was used to fabricate the aerogels instead of 0.135 mL, which is typically called for by the 40-mL standard aerogel recipe (Table 1). The precursor solution could then be processed in the hot press to create aerogels or

left in a capped cuvette and dried slowly under ambient conditions to produce a xerogel.

To fabricate the "10^{-4} M" Rhodamine 6G (R6G) doped aerogels and xerogels used in this research, Rhodamine 6G in the neutral form was purchased from Aldrich Chemical Company, Inc. with a 95% dye content. The R6G was dissolved in reagent-grade methanol to afford a concentration of 10^{-4} M R6G. This R6G in methanol solution was then used in place of the entire volume of methanol required by the recipe. In doing so, a precursor solution was made with a concentration of $<10^{-4}$ M R6G, which could then be used to fabricate "10^{-4} M R6G" doped aerogels and xerogels. We refer to these gels as "10^{-4} M" because this is the R6G concentration before processing. We are not certain what the actual concentration of probe in the aerogels or xerogels actually is. This is because the hot press destroys some of the probe in the fabrication of the aerogels and lowers the actual concentration of probe. In the xerogels, the final product shrinks drastically to afford a higher concentration of probe than what was started with. The inability to know exactly what the concentration of probe is in the sol-gels after processing makes it necessary to refer to the amount of probe by the prefabrication concentration. But it is important to be aware that the final sol-gel does not actually contain the concentration of probe listed.

To fabricate the "$5x10^{-4}$ M" Fluorescein doped aerogels and xerogels used in this research, Fluorescein in the neutral form was purchased from Aldrich Chemical Company, Inc. with a dye content of ~95%, and used without further purification. The Fluorescein was dissolved in reagent-grade methanol to afford a

concentration of $5x10^{-4}$ M Fluorescein. This Fluorescein in methanol solution was then used in place of the normal methanol called for in the recipe noted above in Table 1. In doing so, a precursor solution was made with a concentration of < $5x10^{-4}$ M Fluorescein, which could then be used to fabricate "$5x10^{-4}$ M Fluorescein" doped aerogels and xerogels.

The fabrication of the Rhodamine B gels was done by a former student in the lab, Kathleen Carroll. The fabrication was done in a similar fashion to the other probed gels described here. The probe was introduced into the aerogel in the same manner. The major difference would be in the program settings that she used as they were different from my hot press temperatures, pressures, and dwell times.

Fabrication of Hydrophobic Doped Sol-Gels

In order to create hydrophobic aerogels and xerogels, some of the TMOS in the precursor recipe was replaced by varying amounts of methyltrimethoxysilane (MTMS). The breakdown of the amounts of TMOS and MTMS used to fabricate the hydrophobic sol-gels can be seen below in Table 2.[25]

Table 2: Recipe alteration to afford hydrophobic sol-gels (to replace TMOS in the recipe given in Table 1)

TMOS (mL)	MTMS (mL)	Percent MTMS by volume (%)
8.5	0	0
6.375	2.125	25
4.25	4.25	50
2.125	6.375	75

The remainder of the recipe was the same as in Table 1 except that double catalyst was used for these hydrophobic aerogels, as it was for the standard doped aerogels. That is, the amount of ammonium hydroxide catalyst used in fabricating the probed hydrophobic aerogels was 0.270 mL, not 0.135 mL as listed in Table 1. These sol-gels were created in the same fashion as the standard sol-gels except that part of the TMOS replaced with MTMS to increase the hydrophobicity of the resulting sol-gel monoliths. These hydrophobic aerogels were also doped in the same way as the standard aerogels. The probes were dissolved in methanol to known concentrations and were added to the precursor in place of the normal methanol. The stock solution of Rhodamine 6G was 10^{-4} M and Fluorescein was 5×10^{-4} M in methanol before addition to the precursor mixture. These concentrations were recorded prior to processing the aerogels which means the final hydrophobic aerogels contained a lower concentration of probe. There is no easy way to determine the concentration of the probe in the aerogel monolith, so the doped hydrophobic aerogels are named based on their pre-fabrication concentration.

Rapid Supercritical Extraction

Once the precursor solution was mixed together and stirred for ten minutes, the solution was subjected to Union College's patented Rapid Supercritical Extraction technique (RSCE) using a Tetrahedron hydraulic hot press. In order to fabricate the cuvette-sized aerogel monoliths necessary for spectral analysis a special mold was used consisting of 16 cylindrical wells with a

diameter of 9 mm and with external dimensions of 125 x 125 x 12 mm. This mold was originally designed by Aaron Phillips.[15] A picture of the mold can be seen below in Figure 8.

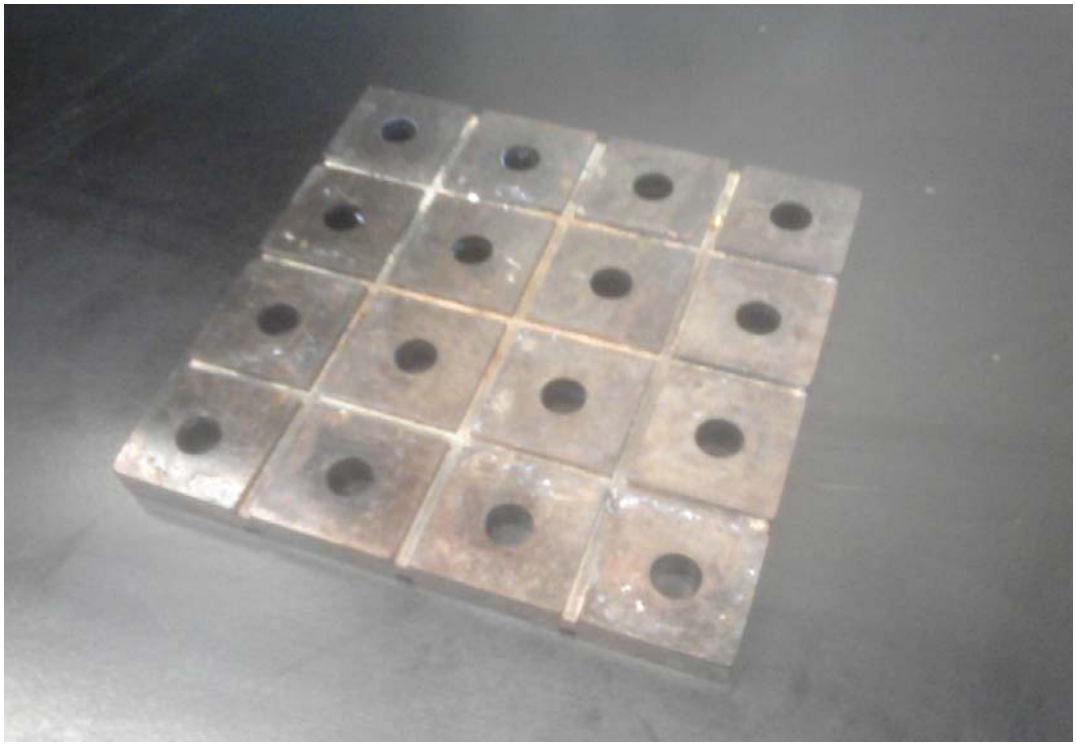

Figure 8: Photograph of 16-well cuvette mold each with a 9-mm diameter used in the fabrication of aerogels via RSCE. External dimensions are 125 x 125 x 12 mm.

First, graphite was placed on the hot press platen, then Kapton, then the mold itself, followed by another layer of Kapton and then graphite. The mold was sealed in the hot press prior to the addition of precursor, in order to ensure that the solution would not leak out when the holes were filled. This was done with a program on the hot press that held the force at 44,500 N (10.0 kips) for a total of ten minutes with the temperature set at 90^{o}F. When this program was finished, an aliquot of the precursor mixture was added to each well, using a pipette to fill to the very top of the well. A fresh piece of Kapton followed by graphite was then

placed on top of the mold and the fabrication program was started. The program used to fabricate the aerogels in the hot press can be seen below in Table 3. In each case, the dwell time is how long the hot press remained at those conditions. The temperature was increased and decreased at 3˚F/min and the force was changed at 4,450 N/min (1 kip/min) in each case before the length of time designated by the dwell time. This should be taken into account when looking at the dwell time of the process. The total time for fabrication from beginning to end is approximately 375 min or 6.25 h.

Table 3: Process parameters for fabrication of aerogels in hot press

Step	**1**	**2**	**3**	**4**	**5**
Temp (^{o}F)	90	510	510	100	end
Force (kN)	125 (28 kips)	125 (28 kips)	4.45 (1 kip)	4.45 (1 kip)	end
Dwell Time (min)	2	30	10	1	end

Table 3 contains the process used to make the standard aerogels discussed above. These standard aerogels are considered hydrophilic due to their inherent properties. In addition to the time table (Table 3), the fabrication of the hydrophobic aerogels required a pre-gelation step. This pre-gelation step was due to the inherent differences in structure between the TMOS and the MTMS. It can be seen from Figure 3 that the MTMS derivative only has three methoxy groups which can polymerize into a framework. This is different from the TMOS which has four methoxy groups that can polymerize. The fact that the MTMS has one less group that is capable of undergoing polymerization slows down the reaction

for kinetic reasons. As you replace groups that can polymerize with groups that cannot, the overall polymerization reaction will be slowed down. This is because fewer of the collisions will afford a polymerization reaction. The pre-gelation step that was required for the MTMS aerogels was accomplished by altering the dwell time on Step 1 to be 480 min long to allow the hydrophobic gels to pre-gel prior to the RSCE. This extended the total time of fabrication from 6.25 h to 14.25 h.

Analysis of Aerogels

The contact angle measurements were accomplished using a 3CCD color vision camera module (Donpisha) to capture the image. ImageJ software was used to analyze the image and determine the contact angle of the water droplet. A water droplet was administered to the surface of the aerogel via an Eppendorf 10 – 100 µL micropipettor. The diameter of the drop was then measured with a ruler. The goal was to keep the droplet size constant for these measurements. Water droplets with diameters in the range of 2.0 to 2.5 mm were utilized in these measurements.

Steady-state fluorescence spectroscopy was performed using a Photon Technology International (PTI) Quantamaster fluorometer with an 810 photomultiplier detector and a LPS-220 lamp power supply. The R6G aerogels were typically excited at 490 nm with an emission slit width of 2 nm and an excitation slit width of 4 nm, and the emission monochromator scanned from 500 to 600 nm. For the Fluorescein aerogels, an excitation wavelength of 490 nm was

also used but the emission slit width was 4 nm, the excitation slit width was 2 nm, and the emission monochromator was scanned from 500 to 580 nm.

In order to analyze these aerogels' response to humidity, several different techniques were utilized. The first technique utilized involved drying the aerogel completely in either a dessicator or the Micrometrics SmartPrep programmable degassing system. The aerogels that were dried for this type of humidity test in a dessicator were left in the dessicator for more than 24 hours. On the SmartPrep degas system, the temperature was set at 50^{o}C and the nitrogen air flow valve was opened. Those aerogels that were dehumidified via a Micrometrics SmartPrep programmable degas system were left on the instrument for more than 24 hours.

Once the aerogel was dried, it was placed in a cuvette in the fluorometer without a cap. The aerogel was then allowed to equilibrate with the air in the room and, therefore, the ambient room humidity. As the aerogel equilibrated with the room humidity, emission scans were taken at intervals to test the response of the molecular probe to the changing relative humidity of the environment. Emission scans were taken every five min for typically 40 min. The beam shutter, which is a shutter that can block the incident beam from reaching the sample, was shut in between each run. This was to prevent photobleaching (the destruction of the probe from light exposure) of the molecular probe. Photobleaching was a potential problem that could interfere with the measurement of the probe's response to humidity and, therefore, make data analysis more difficult.

The subsequent response of the signal to the change in relative humidity experienced by the probe was then plotted in Excel. The resulting plots displayed

signal versus the amount of time that the aerogel was left uncapped. The results were then analyzed as percent change in response to changing humidity as follows:

(Slope of trendline / initial signal response) x 100 = percent response to humidity

Photobleaching was mentioned above as an issue that needed to be minimized. This is because the observed response of the luminescent probes to humidity is a decrease in signal with an increase in relative humidity. In the crude humidity test experiment in which the aerogel is allowed to equilibrate with the room humidity, there will always be an increase in relative humidity experienced by the aerogel. This should always afford a decrease in the observed signal of the molecular probe. This being said, it is uncertain how much of the observed response is due to changes in humidity and how much is due to photobleaching or a deterioration of the molecular probe due to light. A photobleaching test was performed on 0%, 25%, and 50% MTMS aerogels containing both Fluorescein and Rhodamine 6G in order to account for the signal change due to photobleaching. These tests were carried out in the same manner as the humidity scans were except that the aerogel was not dried and was at ambient conditions so the response to humidity would be eliminated. The signal was plotted against the amount of time that passed. This produced an accurate account of the amount of photobleaching experienced by each type of aerogel so that the probe-doped aerogel's response to humidity could be more accurately quantified.

The other method used to analyze the probed aerogel's response to humidity was a humidity apparatus. A schematic view of the humidity apparatus used in this research can be seen below in Figure 9.

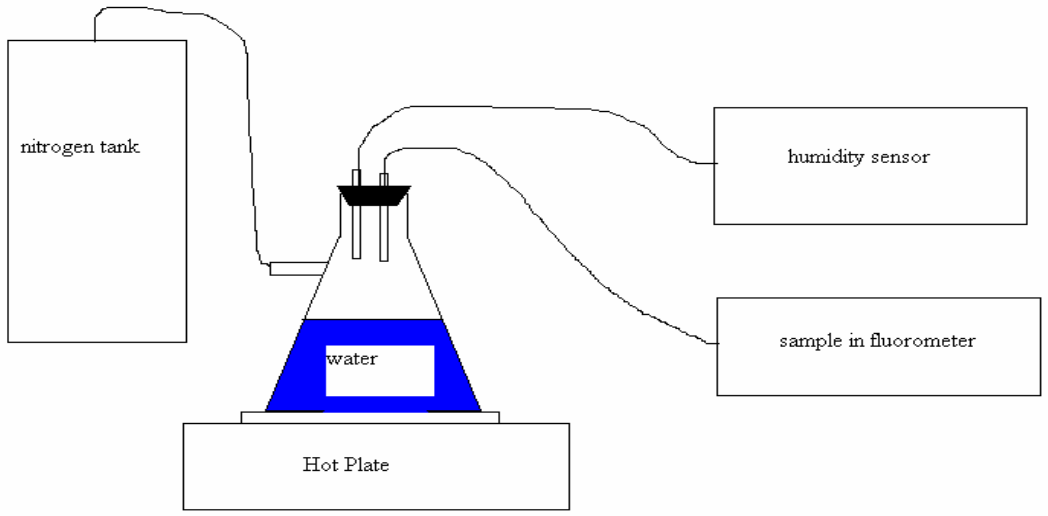

Figure 9: Schematic view of humidity apparatus

In this apparatus, the hot plate heats the water and produces water vapor in the flask. A gentle flow of nitrogen gas enters the flask and forces the water vapor to exit the flask and enter two separate tubes. (It was not possible to measure the exact flow rate of the nitrogen.) The tubes led to an Omega RH85 humidity sensor, to quantify the relative humidity that the aerogel is experiencing, and to the aerogel sample itself in the fluorometer.

Chapter 3: Results

Rhodamine B Humidity Tests

Humidity tests were performed on the Rhodamine B standard aerogels as described in the experimental section by drying them in the Tristar degasser prior to the humidity scan. These humidity tests were conducted for a total of 30 minutes with variable intervals in between each scan. The fluorescence emission intensity versus wavelength was obtained from the humidity test utilizing the Quantamaster fluorometer instrument located in the basement aerogel lab N007. Representative fluorescence emission spectra obtained for these tests can be seen below in Figure 10 for a 3.5 x 10^{-5} M Rhodamine B (RB) aerogel sample.

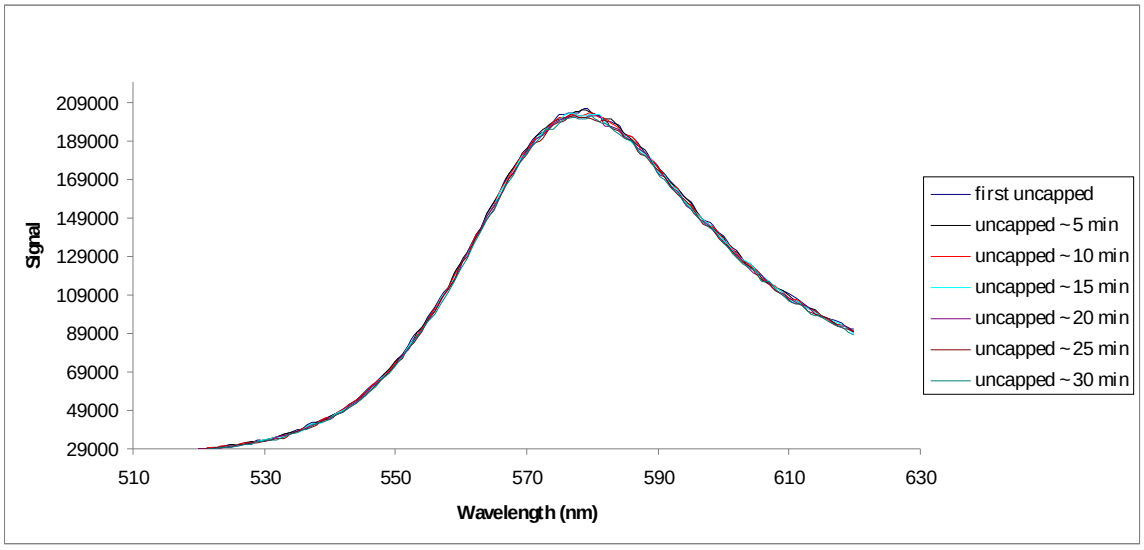

Figure 10: Fluorescence emission spectra for a 3.5 x 10^{-5} M Rhodamine B aerogel excited at 420 nm going from Tristar degasser to room humidity. The aerogel was dried via heat and nitrogen gas. It was then placed in the fluorometer without a cap on the cuvette and the aerogel was allowed to equilibrate to room humidity. This was to simulate going from a dry environment to a humid one (increasing humidity).

From the spectra in Figure 10, it was difficult to determine the response of the emission intensity with respect to changing humidity so the data obtained from these spectra were plotted in Microsoft Excel for further analysis. The Excel plot depicting the signal intensity at 579 nm versus the amount of time uncapped for the same Rhodamine B aerogel can be seen below in Figure 11. A straight line is shown for visual aid but there is no fundamental reason why the response should be linear.

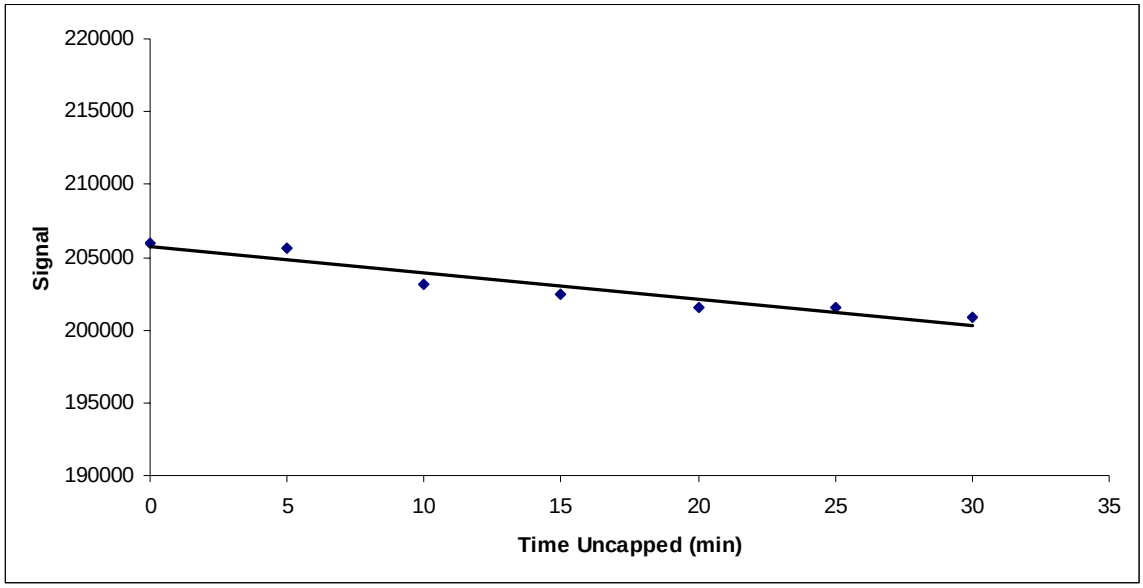

Figure 11: Plot of signal intensity at 579 nm versus time uncapped for an RB aerogel sample excited at 420 nm. The aerogel was initially dry at time zero and experienced increasing humidity as time went on and the aerogel equilibrated with room humidity. The response of the signal should be the response to an increase in humidity as time progresses. The trend line is shown for visual clarity but there is no fundamental reason to suspect that the response of the probe to humidity should be linear.

It is apparent from this graph that there is a slight decrease in emission signal intensity with the amount of time that the aerogel was left uncapped in the fluorometer. A percent response, using the slope divided by the initial signal then multiplied by 100, was calculated to be -0.087% for this test.

Rhodamine 6G Humidity Tests

Humidity tests were performed on the Rhodamine 6G standard aerogels in the way described in the experimental section by drying them in a dessicator prior to the humidity scan. These humidity tests were conducted for a total of 95 minutes with variable intervals in between each scan. The fluorescence emission intensity versus wavelength was obtained from the humidity test utilizing the Quantamaster fluorometer instrument located in the basement aerogel lab N007. Representative fluorescence emission spectra obtained for these tests can be seen below in Figure 12 for a 100% TMOS 10^{-4} M Rhodamine 6G aerogel labeled "M15."

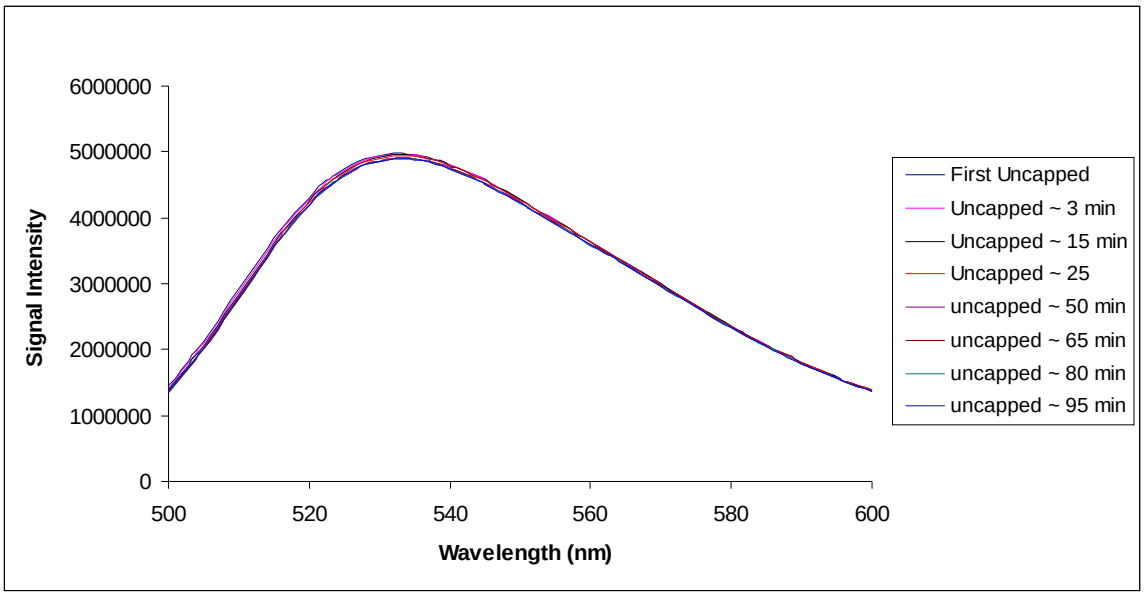

Figure 12: Fluorescence emission spectra for M15 10^{-4} M 100% TMOS aerogel excited at 490 nm. The aerogel was dried in a dessicator, placed in a cuvette within the fluorometer, and left uncapped throughout the scans. This was meant to simulate going from a dry environment to one of increased humidity as the aerogel equilibrated with the room environment. As time progressed, the signal of the probe should have changed, corresponding to increasing humidity.

At first glance it does not appear that the fluorescence emission intensity is changing at all with respect to changing humidity. In order to determine the exact response of the fluorescence emission signal to changing humidity, the signal intensity was plotted against the time left uncapped. The Excel plot depicting the signal intensity at 533 nm versus the amount of time uncapped for the same M15 aerogel can be seen below in Figure 13. The trend line is displayed for visual aid and it should be noted that there is no fundamental reason why the response should be linear.

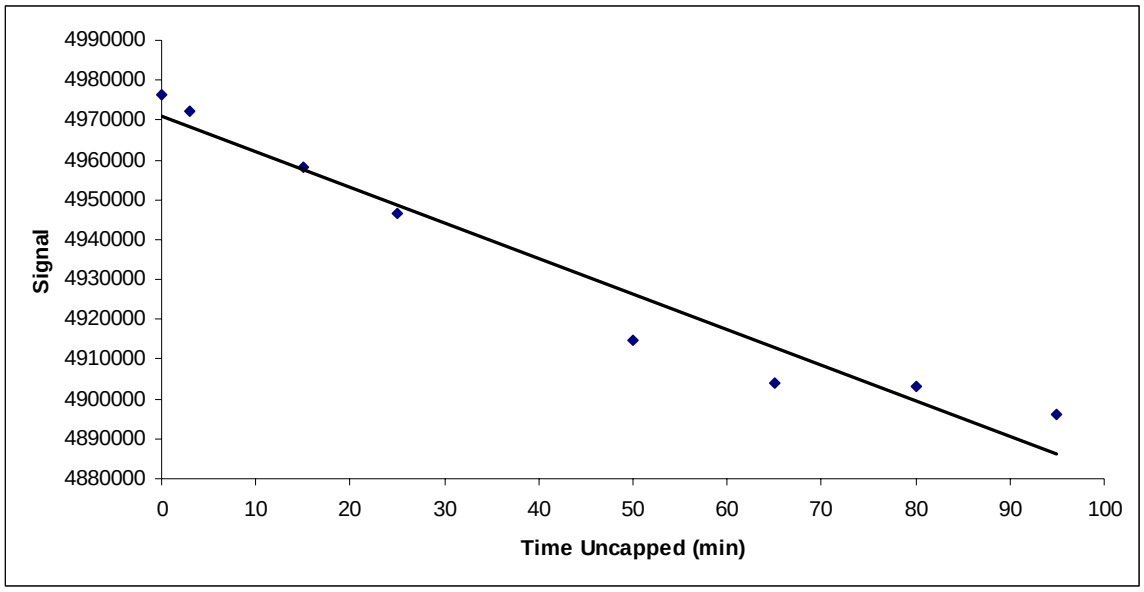

Figure 13: Excel plot of signal intensity at 533 nm versus time uncapped for 10^{-4} M Rhodamine 6G 100 % TMOS aerogel sample M15 excited at 490 nm. The aerogel was initially dry at time zero and was placed in a cuvette uncapped within the fluorometer for the run. This was meant to equilibrate the aerogel with the room environment and to simulate an increase in humidity throughout the run. The response of the probe seen is a response due to increasing humidity experienced by the probe.

It is observed in this plot that there is an apparent decrease in the response of the signal intensity to the amount of time that the aerogel sample was left uncapped in the fluorometer. This corresponds to a decrease in the signal with an increase in

humidity. In order to analyze the change in signal, the percent response to humidity signal was calculated. The calculated response in the humidity tests, using the slope divided by the initial signal then multiplied by 100, for the Rhodamine 6G 100% TMOS samples can be seen below in Table 4.

Table 4: Percent change in overall signal for the humidity tests for the 100% TMOS Rhodamine 6G aerogels

Rhodamine 6G sample	% response
M13	-0.034
M15	-0.018

Humidity tests were performed on the Rhodamine 6G hydrophobic aerogels in the way described above by drying them in a dessicator prior to the humidity scan. The only difference from the 100% TMOS aerogel humidity tests was that these were conducted for a total of two hours with 20-minute intervals between each scan. The fluorescence emission intensity versus wavelength was obtained from the humidity test utilizing the fluorometer instrument. Representative fluorescence emission spectra obtained for these tests can be seen below in Figure 14 for a 50% TMOS / 50% MTMS 10^{-5} M Rhodamine 6G aerogel labeled “F10”.

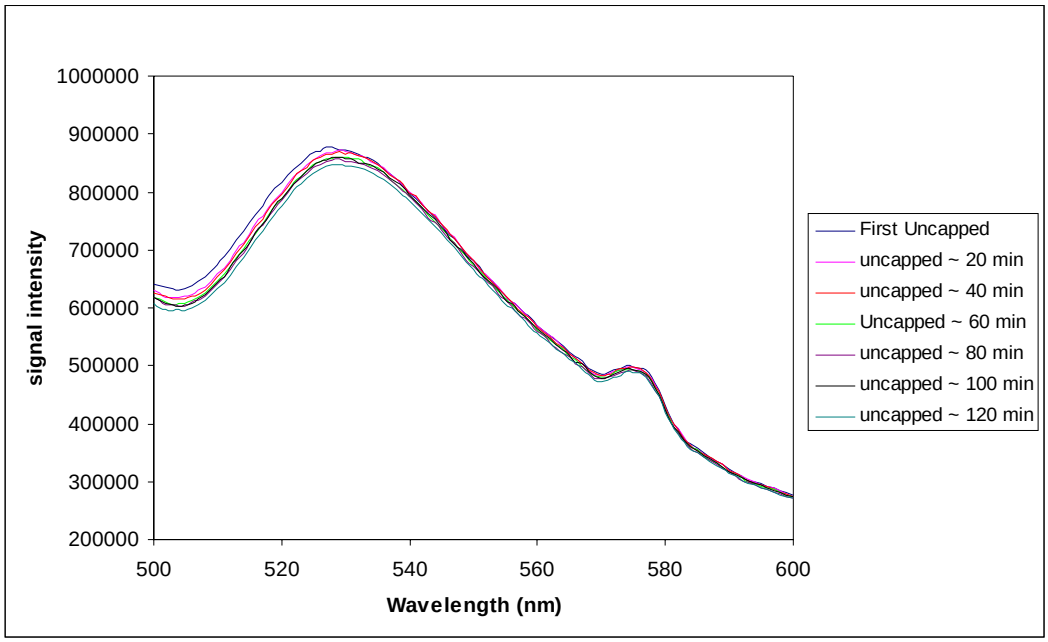

Figure 14: Fluorescence emission spectra for F10 (50 %TMOS / 50% MTMS) 10^{-5} M Rhodamine 6G hydrophobic aerogel excited at 470 nm. The aerogel was dried in dessicator at the beginning of the scan and was placed in a cuvette uncapped for fluorescence measurements. The aerogel was allowed to equilibrate with the room environment throughout the scan. This was to simulate increasing humidity experienced by the aerogel. As time progressed the probe response was due to an increase in humidity.

It was difficult to determine the response of the emission intensity with respect to changing humidity so the data obtained from these spectra was plotted in Microsoft Excel for further analysis. The Excel plot depicting the signal intensity at 533 nm versus the amount of time uncapped at a wavelength for the same F10 aerogel can be seen below in Figure 15.

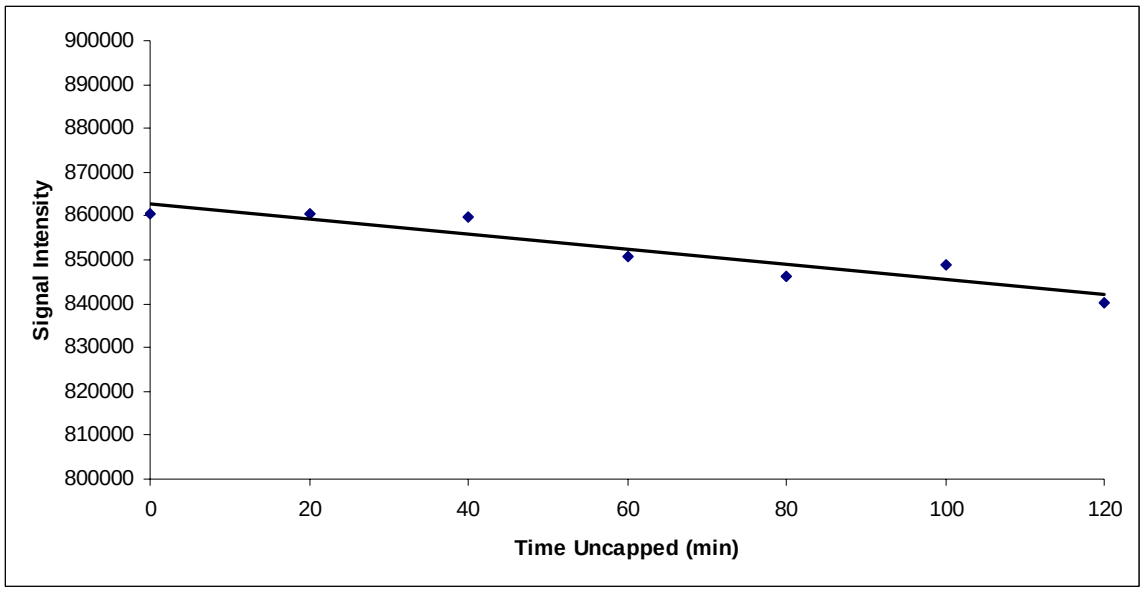

Figure 15: Excel plot of signal intensity versus time uncapped at 533 nm for (50 %TMOS / 50% MTMS) 10^{-5} M Rhodamine 6G hydrophobic aerogel excited at 470 nm. The aerogel was initially dried at time zero in a dessicator, placed in a cuvette, and fluorescence was conducted with the cuvette uncapped to allow the aerogel to equilibrate with room humidity. This was to simulate going from a dry environment to one of increasing humidity. The response of the probe in this test should be the response to an increase in humidity.

It is apparent from this graph that there is a slight decrease in emission signal intensity with the amount of time that the aerogel was left uncapped in the fluorometer. A percent response, using the slope divided by the initial signal then multiplied by 100, of -0.020% was calculated for the above humidity test.

Fluorescein Humidity Tests

The humidity tests for the Fluorescein aerogels were originally performed by drying the aerogels in a dessicator and then carried out as described in the experimental section. These humidity tests were conducted for a total of 50 minutes with 5 minute intervals in between each scan. The fluorescence emission intensity versus wavelength was obtained from the humidity test utilizing the

fluorometer instrument. Representative fluorescence emission spectra obtained for these tests can be seen below in Figure 16 for a 100% TMOS 5 x 10^{-4} M Fluorescein aerogel labeled N3. The emission spectra for all the dessicator-dried samples looked similar to the ones below.

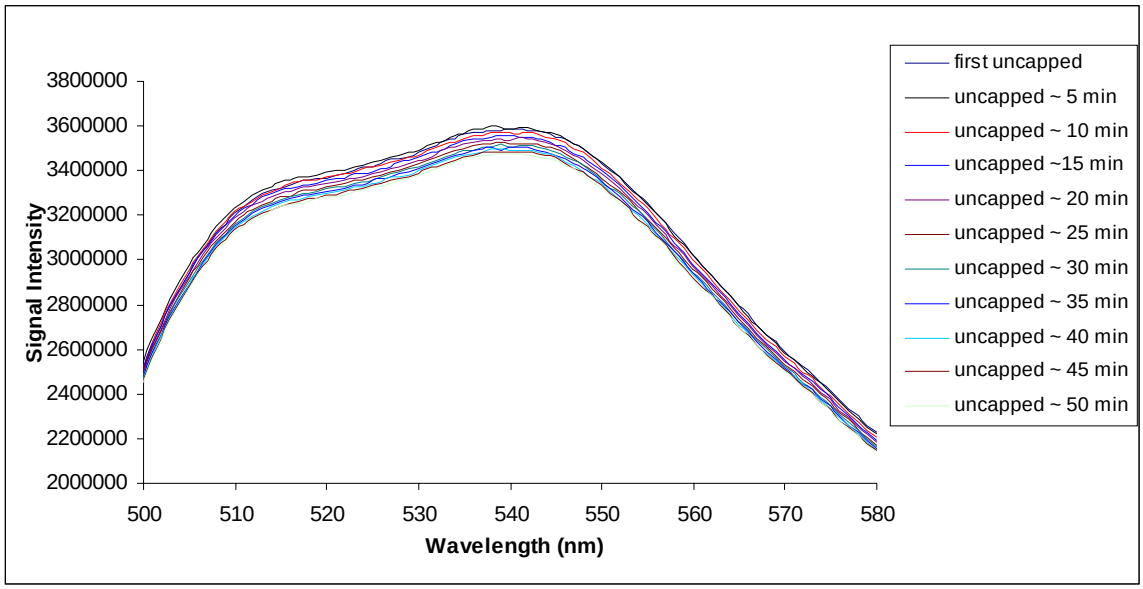

Figure 16: Fluorescence emission spectra for N3 (100%TMOS) 5 x 10^{-4} M Fluorescein aerogel excited at 468 nm. The aerogel was dried in a dessicator and fluorescence was conducted on the aerogel in an uncapped cuvette. This was to allow the aerogel to equilibrate with room humidity and to simulate an increase in humidity experienced by the probe. Response of probe observed should be a response to an increase in humidity.

It is apparent from these emission spectra that there is a decrease in the signal intensity over time. In order to get a better understanding of how much the intensity was changing, a plot of signal intensity at 541 nm versus time was created in Excel. The plot for the N3 sample can be seen below in Figure 17.

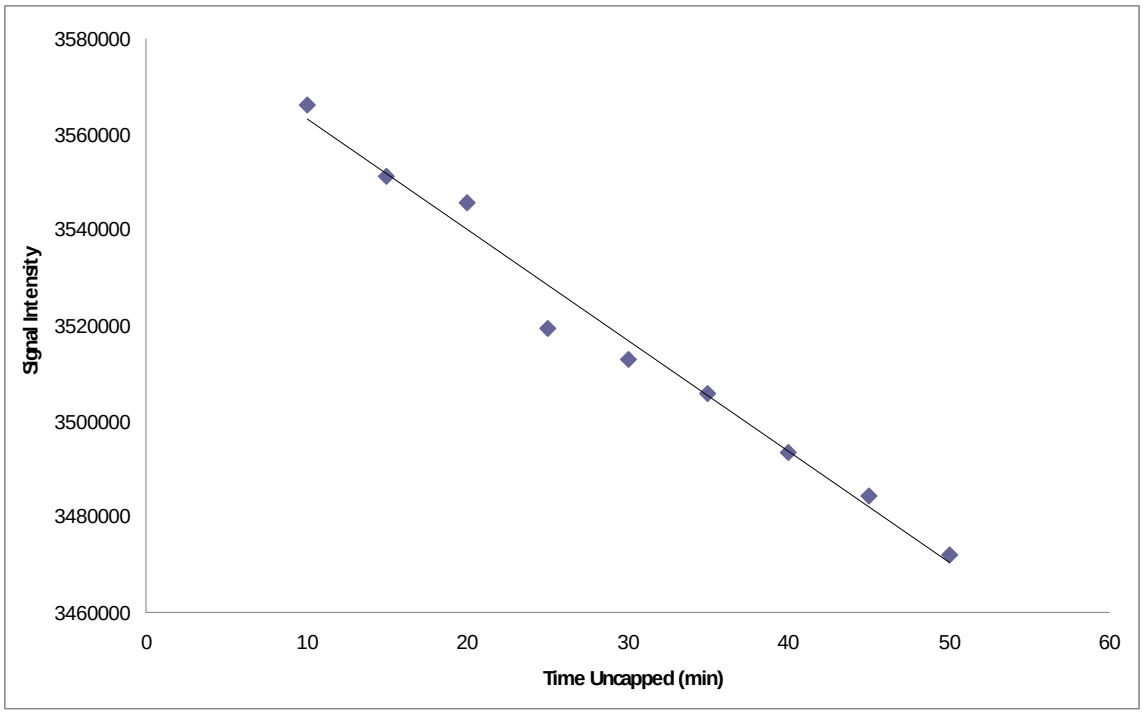

Figure 17: Excel plot of signal intensity versus time uncapped at 541 nm for sample N3 (100% TMOS) 5×10^{-4} M hydrophilic aerogel excited at 468 nm. Sample was dried initially at time zero and was then allowed to equilibrate to room humidity within an uncapped cuvette during fluorescence measurements. This was to simulate an increase in humidity experienced by the aerogel. The response seen should be a response of the probe to increasing humidity.

It is apparent from this graph that there is a slight decrease in emission signal intensity with the amount of time that the aerogel was left uncapped in the fluorometer. This graph is representative of a typical plot for all aerogels, hydrophobic and hydrophilic, dried via the dessicator. A percent response, using the slope divided by the initial signal then multiplied by 100, was calculated for the samples tested and their values can be seen below in Table 5. It was always the case that there was a decrease in signal intensity with an increase in humidity experienced by the aerogel.

Table 5: Percent response to humidity for 5 x 10^{-4} M Fluorescein aerogels dried in a dessicator

Sample	% TMOS / MTMS	% response
N14	100 / 0	-0.027
N14	100 / 0	-0.032
N14	100 / 0	-0.007
O16	50 / 50	-0.073

The humidity tests were then performed by drying the aerogel using the Tristar degassing system instead of the dessicator. The emission spectra of the aerogels dried in this manner looked very similar to the ones in Figure 16. The response of the aerogels to humidity in each case was plotted in Excel in a similar manner to that presented in Figure 17. It was typical that the response to humidity would be a loss in the total emission signal as the humidity increased. The calculated percent loss of signal due to humidity from each test conducted can be seen below in Table 6.

Table 6: Response to humidity for the aerogels dried via the Tristar degasser system

Sample	TMOS/MTMS	Humidity Test %
N6	100 / 0	-0.131
N6	100 / 0	-0.102
N6	100 / 0	-0.165
P16	75 / 25	-0.045
P16	75 / 25	Positive Slope / No % loss
O13	50 / 50	Positive Slope / No % loss
O13	50 / 50	Positive Slope / No % loss

Fluorescein Photobleaching

The photobleaching results for the aerogels of varying degrees of hydrophobicity were also determined. The fluorescence emission spectra of these tests were similar looking to the previous Fluorescein emission spectra shown. In each case the signal decreased as time elapsed. The signal intensity was then plotted in Excel the same way it was done for the humidity tests. The percent loss in signal due to photobleaching was calculated, using the slope divided by the initial signal then multiplied by 100, for the different aerogels of varying degrees of hydrophobicity. These results can be seen below in Table 7.

Table 7: Photobleaching results for 5 x 10^{-4} M Fluorescein aerogels. Three values are listed for P16 because it was tested three times. Two values are listed for N6 because it was tested twice. The O13 sample was only tested once.

Sample	TMOS/MTMS	Photobleaching %
N6	100 / 0	-0.066 / -0.066
P16	75 / 25	-0.073 / -0.093 / -0.080
O13	50 / 50	-0.047

Fluorescein Humidity Tests Continued

During the course of this research, it was suspected that the nitrogen gas from the Tristar degasser was not flowing out and into the sample. The tube where the nitrogen comes out was placed in a beaker of water and no bubbles formed. The valves were adjusted and bubbles appeared in the water, confirming that the nitrogen gas was now flowing into the sample tube. Subsequently, the humidity tests for these gels were reexamined. These humidity tests were conducted for a total of 50 minutes with 5-minute intervals in between each run.

The fluorescence emission intensity versus wavelength was obtained from the humidity test utilizing the fluorometer instrument. Fluorescence emission spectra obtained for these tests can be seen below in Figure 18 for a 100% TMOS 5 x 10^{-4} M Fluorescein aerogel labeled N2. The emission spectra for all the Tristar dried samples, once the nitrogen gas flow was confirmed, looked similar to the ones below.

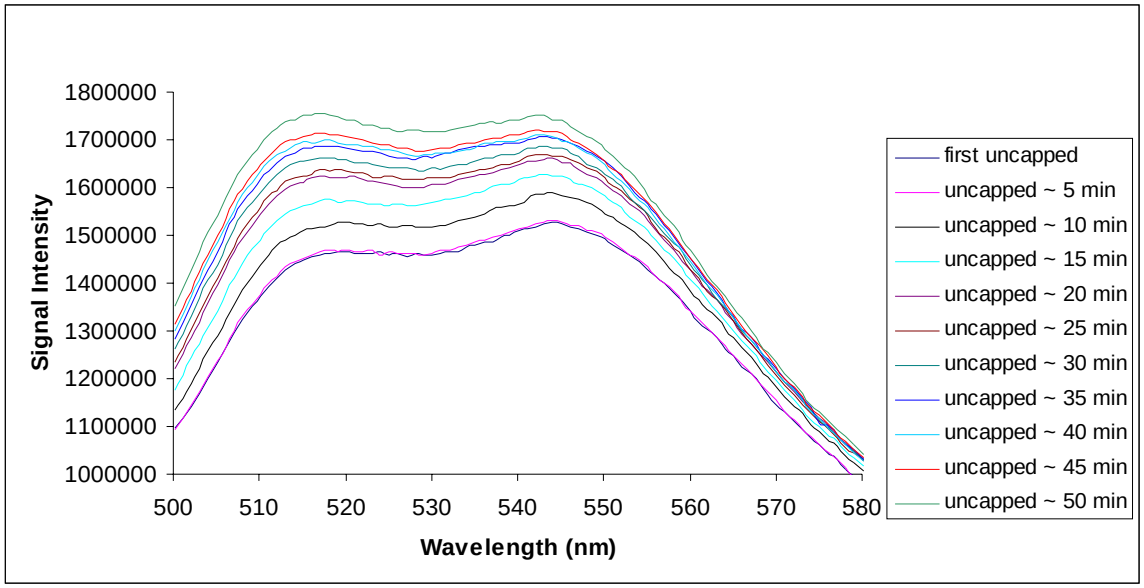

Figure 18: Fluorescence emission spectra for N2 (100%TMOS) 5 x 10^{-4} M fluorescein aerogel excited at 490 nm. The aerogel was initially dried and then fluorescence emission of the sample was obtained in an uncapped cuvette. This allowed the aerogel to equilibrate with room humidity and simulated an increase in humidity over time. The response seen is a response of the probe to increasing humidity.

There is obviously a response to the changing humidity displayed in these emission spectra. As the time elapsed and the humidity that the aerogel experienced increased, the signal also increased. This positive response to the increase in humidity is opposite of what was previously observed. In order to quantitate the response of the probe to the increasing level of humidity, the data was plotted as signal intensity at 544 nm versus time uncapped in Excel. The plot

for the N_2 humidity test displayed above in Figure 18 can be seen below in Figure 19.

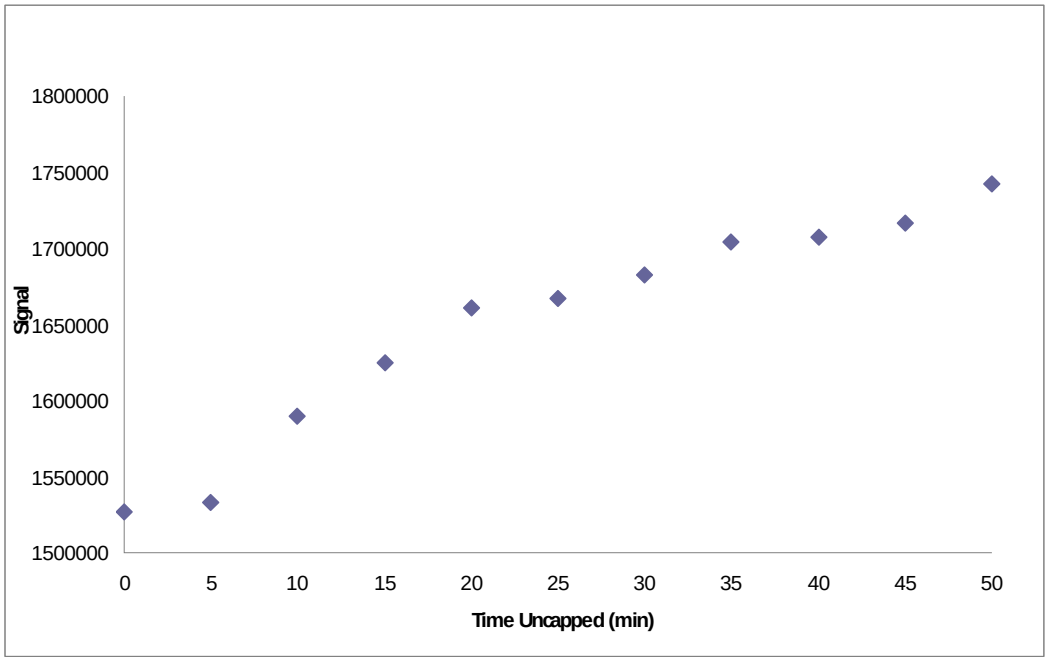

Figure 19: Excel plot of signal intensity versus time uncapped at 544 nm for sample N2 5 x 10^{-4} M Fluorescein aerogel excited at 490 nm. The aerogel was initially dried and then fluorescence emission of the sample was obtained in an uncapped cuvette. This allowed the aerogel to equilibrate with room humidity and simulated an increase in humidity over time. The response seen is a response of the probe to increasing humidity.

The fluorescence emission spectra for the O13 (50% TMOS / 50% MTMS) and the P16 (75% TMOS / 25% MTMS) looked like the emission spectra in Figure 18. The signal intensity increased as the time the aerogel was left uncapped increased. The response of these samples to the increase in humidity was also plotted as signal intensity versus time uncapped in Excel. The two plots for O13 and P16 can be seen below in Figures 20 and 21 respectively.

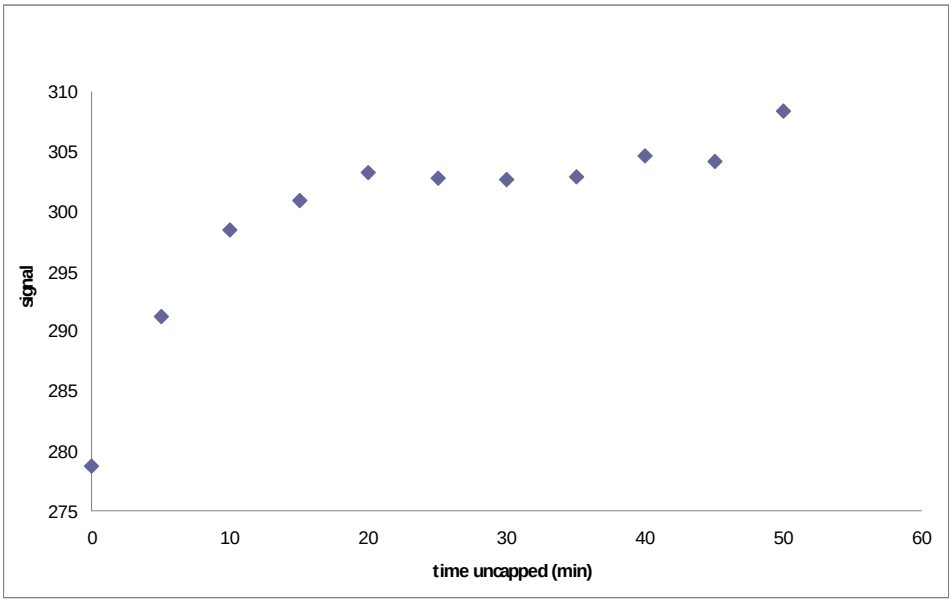

Figure 20: Excel plot of signal intensity versus time uncapped at 545 nm for sample O13 5 x 10^{-4} M Fluorescein aerogel excited at 490 nm. The aerogel was initially dried and then fluorescence emission of the sample was obtained in an uncapped cuvette. This allowed the aerogel to equilibrate with room humidity and simulated an increase in humidity over time. The response seen is a response of the probe to increasing humidity.

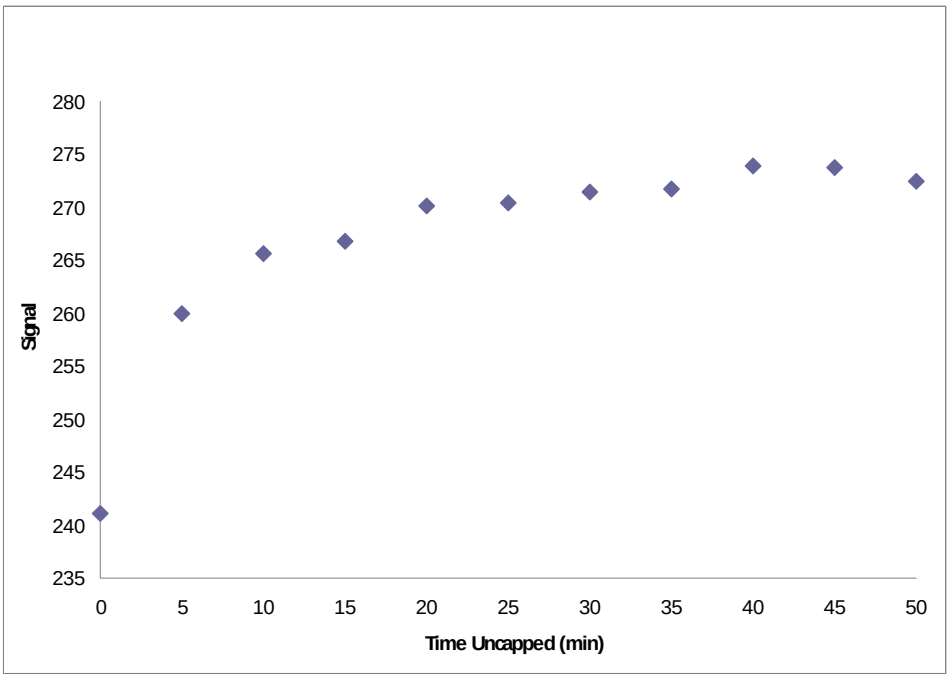

Figure 21: Excel plot of signal intensity versus time uncapped at 544 nm for sample P16 5 x 10^{-4} M Fluorescein aerogel excited at 490 nm. The aerogel was initially dried and then fluorescence emission of the sample was obtained in an uncapped cuvette. This allowed the aerogel to equilibrate with room humidity and simulated an increase in humidity over time. The response seen is a response of the probe to increasing humidity.

The response of the signal to the change in humidity was not a linear one so the previous method of determining the percent response will not apply here. Instead, the response was quantified as a simple percent change between the initial and final signal intensities. The percent change in signal corresponding to the response to humidity for N2, O13, and P16 can be seen below in Table 8.

Table 8: Percent change in signal intensity from initial to final signal for N2, N10, O13, O14, P15, and P16 aerogels. Those samples with two values were tested on two separate occasions.

Sample	TMOS/MTMS	% Change in Signal
N2	100 / 0	+14.14 / +13.80
N10	100 / 0	+12.50
P16	75 / 25	+13.58 / +16.73
P15	75 / 25	+13.7
O14	50 / 50	+7.00
O13	50 / 50	+10.61

Humidity Apparatus

The first humidity test conducted on the humidity apparatus was performed on sample A16 100% TMOS 10^{-5} M Rhodamine 6G. This aerogel was left in the fluorometer while the humidity was varied using the apparatus and the resulting fluorescence emission signal was recorded. The emission spectra for this aerogel can be seen below in Figure 22.

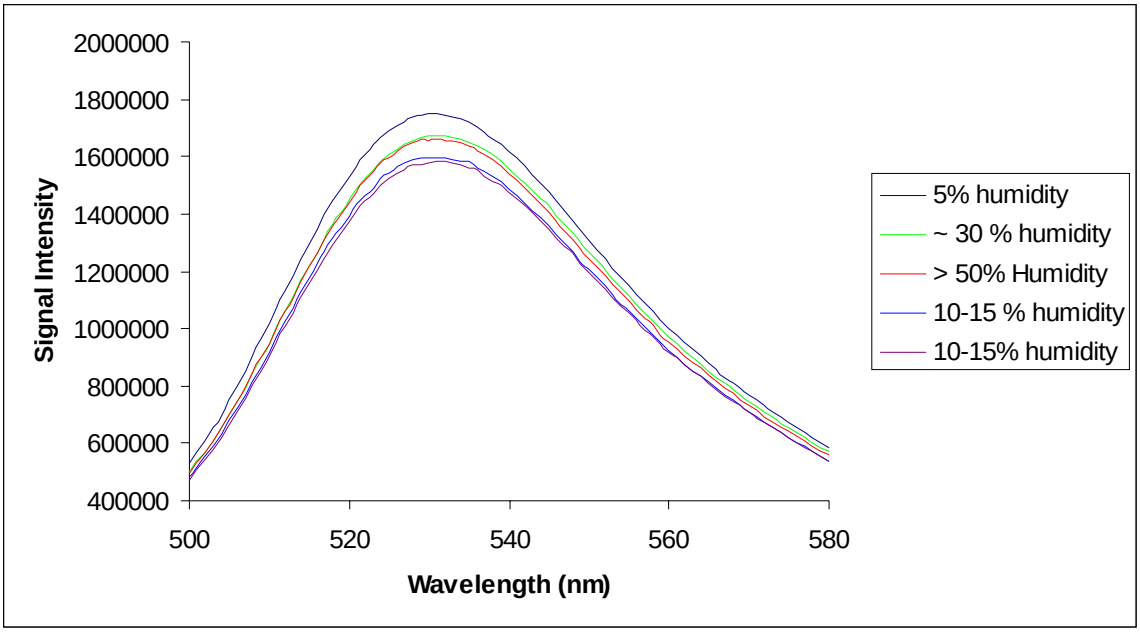

Figure 22: Emission spectra of A16 100% TMOS 10^{-5} M Rhodamine 6G Fluorescein aerogel excited at 490 nm. This test was conducted by varying humidity conditions using humidity apparatus. The humidity was altered via changing the flow of nitrogen and the amount of water vapor produced in the system.

It can be seen from the above spectra that there is no clear trend observed relating the intensity of the emission signal to the percent relative humidity experienced in the room. The emission signal begins high, then drops with increasing humidity but then stays at a low signal when the humidity is reduced again. In order to test if the nitrogen gas used in the humidity apparatus affected the signal observed, the nitrogen gas flow was varied on an aerogel sample that was at ambient conditions. This eliminated the emission signal response due to humidity and just focused on the affect the flowing nitrogen gas had on the aerogel sample. The nitrogen was turned on at the specified rate and then the valve would be closed in order to obtain the emission spectra to see if the nitrogen had an affect on the signal. The fluorescence emission scans depicting this test for N6 100% TMOS 10^{-5} M Fluorescein aerogel can be seen below in Figure 23.

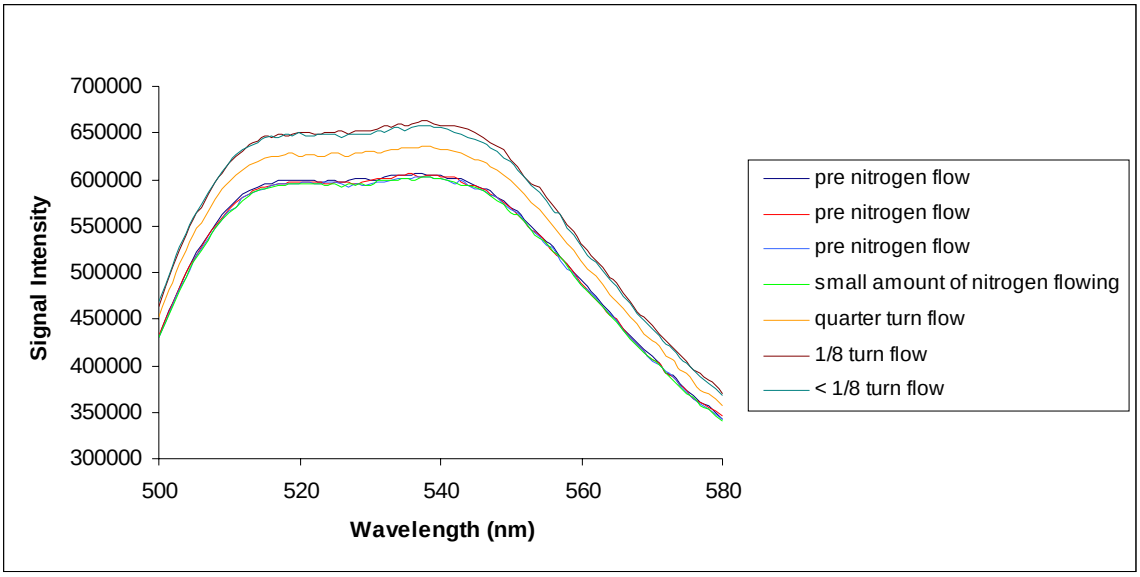

Figure 23: Emission scan of N6 100% TMOS 5 x 10^{-4} M Fluorescein aerogel excited at 490 nm. This was a nitrogen gas test using the humidity apparatus. The nitrogen was altered without humidity present. The response seen is not due to variations in humidity but variations in the flow of nitrogen through the apparatus.

It can be seen from the above fluorescence emission spectra in Figure 23 that the signal remained unchanged when there was no nitrogen, or a very small amount of nitrogen, flowing into the cuvette containing the aerogel sample. It is also evident that opening the nitrogen valve a quarter turn and then collecting a scan had an effect on the resulting emission. It is also seen that opening the valve only an eighth of a turn also had an effect on the resulting emission spectra. Lastly, it can be seen that opening the valve less than an eighth of a turn had no profound effect on the resulting emission spectra of the aerogel sample.

To attempt to reduce the effect of the flowing nitrogen on the fluorescence emission intensity, sample N16 100% TMOS 5 x 10^{-4} M Fluorescein aerogel was hot glued to the bottom of the cuvette. The nitrogen flow was then altered in the apparatus without any water present. This isolated the conditions to just flowing

nitrogen and not changing humidity. The resulting fluorescence emission spectra can be seen below in Figure 24.

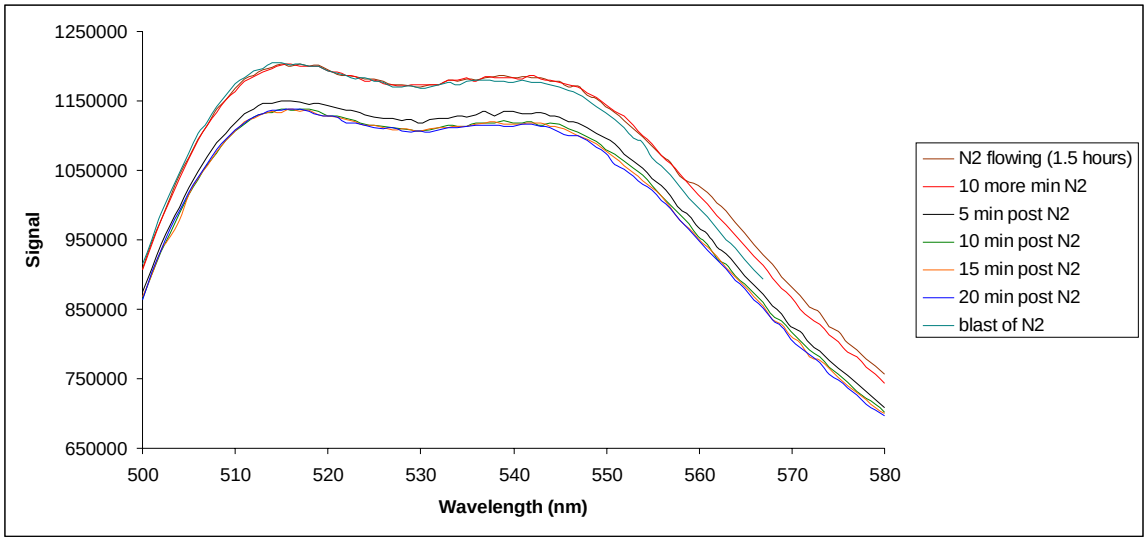

Figure 24: Fluorescence emission spectra for N16 100% TMOS 5 x 10^{-4} M Fluorescein aerogel excited at 490 nm. Emission scans were collected using the apparatus while changing the flow of nitrogen but not the humidity. The change in signal observed was due to the periods in between nitrogen flow.

From the emission spectra in Figure 24, it can be seen that the nitrogen flow itself had no effect on the resulting emission scan as depicted by the repeat emission at the highest signal collected during flowing nitrogen. The emission signal did not change with continuously flowing nitrogen. When the nitrogen was turned off, the signal dropped steadily. When a brief shot of nitrogen was then reapplied, the signal immediately returned to the initial high signal. This drop in signal after nitrogen exposure, and assumed drying, is different from that previously observed in Figure 9 for the Fluorescein aerogels. In order to test this response, a time based emission scan was performed on the N16 100% TMOS 5 x 10^{-4} M Fluorescein aerogel in the humidity apparatus. The resulting scan can be seen below in Figure 25.

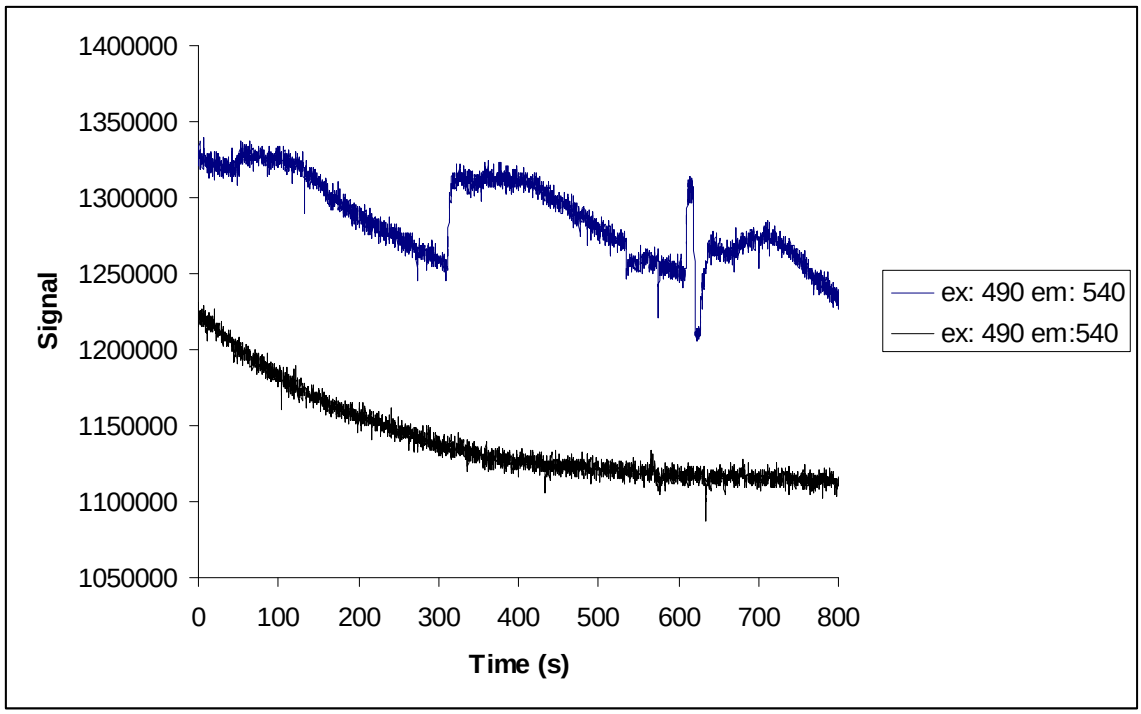

Figure 25: Time based emission scan of N16 100% TMOS 5 x 10^{-4} M Fluorescein aerogel. **Blue line:** The nitrogen was flowing up until 100 s then turned off. Nitrogen turned back on at 300 s. Nitrogen turned off again at 400 s. Humidity on at 600 s. Humidity left on through remainder of scan. **Black line:** humidity left on and continuously acquired emission scans at a humidity of about 90%.

Nitrogen was flowing continuously until 100 s when it was shut off and the signal dropped (blue line in Figure 25). The nitrogen was turned back on again at 300 s and the signal immediately shot back up. The nitrogen was turned back off at 400 s, at which point the signal dropped again. The humidity apparatus was applied at 600 s at a humidity of 90% and the signal dropped. The humidity was left on and the signal was obtained for an additional 800 s (black line in Figure 25). This line shows a decrease in emission intensity with the probe experiencing an increase in humidity. The signal eventually levels out. The contradictory response of Fluorescein signal decreasing in response to an increase in humidity is observed here as well.

Sessile Water Droplet Contact Angles

A representative photo of the contact angle analysis of a sessile water droplet can be seen below in Figure 26. This image is of the O13 (50% TMOS / 50% MTMS) 10^{-5} M Fluorescein aerogel.

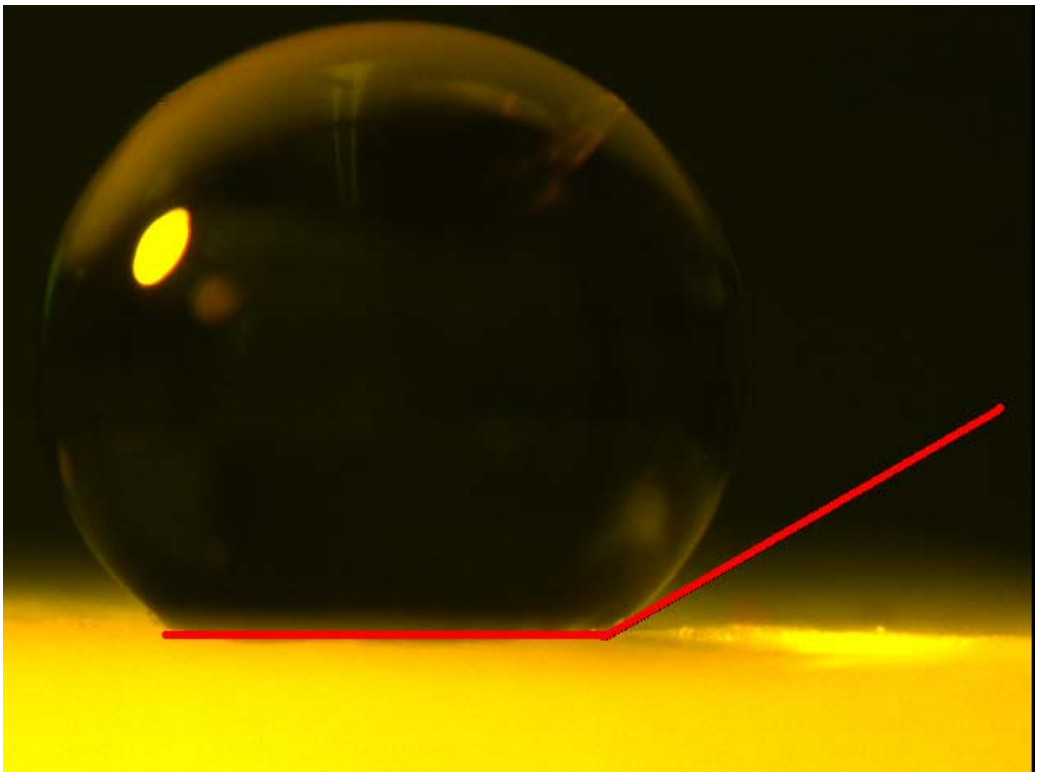

Figure 26: Contact angle measurement for sample O13 (50% TMOS / 50% MTMS) 10^{-5} M aerogel. The lines were drawn separately by free hand in the program Image J. The resulting angle formed by the lines was then analyzed in Image J as well. The resulting data was the contact angle measurement obtained for the aerogel samples.

This image was analyzed in ImageJ and the program calculated the angle that was drawn onto the image. A listing of the samples tested can be seen below in Table 9. This list includes both probe-doped and non-probe-doped hydrophobic and standard gels. It should be noted that the repeat measurements

are of the same image and the drawing and measuring of the angle was the only thing repeated. It should also be noted that there are no "N" 100% TMOS 10^{-5} M Fluorescein contact angles listed as it was impossible to get the water droplet to remain on the surface of the aerogel. The water droplet immediately soaked into the aerogel, destroying the sample, so it was not feasible to obtain an image of the droplet on any of the 100% TMOS aerogels that contained probe.

Table 9: Calculated sessile water droplet contact angle measurements for various aerogel samples

Sample	TMOS / MTMS	Contains Probe?	Measured Contact Angle
P 15	75 / 25	yes	145.5 / 146.2 / 145.1
O 13	50 / 50	yes	149.8 / 149.3
O 15	50 / 50	yes	156.4 / 156.3 / 155.6
U5	100 / 0	no	124.9 / 124.8
V1	75 / 25	no	142.5 / 143.8 / 143.2
T16	50 / 50	no	150.3 / 151.7 / 151.7

It was then noticed that the formatting of the image was set to a wide screen view which distorted the droplet image. The droplet appeared to be wide and oblong instead of nearly spherical. This was suspected to lead to incorrect contact angle measurements and the program had to be altered. The formatting of the image capturing program was changed and new results were obtained for the contact angles of sessile droplets. These new results can be seen below in Table 10. It should be noted that the reformatted images may appear to have smaller contact angles but they are quite similar in magnitude. It turns out that the reformatting did not have a profound effect on the measured contact angle. The

contact angles obtained from the reformatted images were used in order to ensure better accuracy.

Table 10: Calculated sessile water droplet contact angle measurements for various aerogel samples after the image capturing software had been reformatted

Sample	TMOS / MTMS	Contains Probe?	Measured Contact Angle
P13	75 / 25	yes	139.9 / 139.4
P14	75 / 25	yes	142.5 / 144.3
O13	50 /50	yes	156.5 / 154.1
U12	100 / 0	no	117.6 / 112.6
V8	75 / 25	no	138.1 / 141.7
V12	75 / 25	no	141.5 / 138.9
T4	50 / 50	no	154.4 / 156.0 / 155.5
T16	50 / 50	no	153.2 / 152.8

Chapter 4: Discussion

Rhodamine B

From the fluorescence emission scan in Figure 10, it was clear that the presence of Rhodamine B in the aerogel was detected via fluorescence. This meant the dye did not completely decompose during the fabrication process and that it was successfully incorporated into the aerogel. This led to the conclusion that Rhodamine B was a viable option for optical probes in silica-based aerogels fabricated using Union's RSCE process.

The plot depicting the 100% TMOS 3.5×10^{-5} M Rhodamine B signal response to humidity over time (Figure 11) shows that there was a slight decrease in signal with an increase in humidity when the aerogel was dried using the Tristar degassing system. Otsuki and Adachi reported that there should be an increase in absorption of Rhodamine B with an increase in humidity.[18] We assumed that this increase in absorption would lead to an increase in fluorescence in the presence of an increase in humidity. Based on the assumption made, the decrease in fluorescence intensity of Rhodamine B with an increase in humidity does not follow the logic adapted from Otsuki and Adachi.[18] However, the observed decrease in signal might not be significant as it was less than a 0.1% change in the overall signal.

The combination of the response opposite to that expected based on the literature and the insignificance in the overall change in response led to the conclusion that Rhodamine B was not a suitable relative humidity probe to detect

the extent of water vapor permeation in hydrophobic and hydrophilic aerogels. As of now, no further testing is planned for the implementation of Rhodamine B as a humidity sensitive probe in this project.

Rhodamine 6G

From the fluorescence emission spectra in Figures 12 and 14, it was clear that Rhodamine 6G was present and could be detected within the aerogels. This meant the dye was incorporated into the aerogel and was not completely decomposed during the fabrication process. This led to the conclusion that Rhodamine 6G was a viable selection as an optical probe for silica aerogels fabricated using Union College's RSCE method.

From Figure 13, it is apparent that there was a decrease in the emission signal of Rhodamine 6G in the 10^{-4} M R6G 100% TMOS aerogel with an increase in relative humidity when the R6G-doped aerogel was dried in a dessicator. This was in agreement with Choi and Tse, who reported that with an increase in relative humidity, there was an observed decrease in the emission signal intensity when Rhodamine 6G is incorporated within a gelatin matrix.[17] Choi and Tse observed a drop from a relative emission intensity of about 2.5 to about 1.9 going from 0 to 100% RH humidity.[17] The decrease in signal due to the increase in humidity observed in this research was deemed to be insignificant as it was under 0.1% for all humidity trials involving Rhodamine 6G (see Table 4). This insufficient response of the signal to changing humidity in this research led to the

conclusion that this molecular probe would not be a viable option for probing the extent of water vapor permeation in hydrophobic and hydrophilic aerogels.

Figure 15 shows a slight decrease in the observed signal response of an R6G-doped hydrophobic aerogel to humidity when the aerogel was dried in the dessicator. This, again, was in agreement with the response found by Choi and Tse as Rhodamine 6G was reported to have a decrease in emission intensity with an increase in humidity when incorporated into a gelatin matrix along with an ethylene glycol-water mixture .[17] The overall change in signal of the Rhodamine 6G observed in this research was less than 0.1% again. This is not significant enough to be considered an observed response of the emission to the change in humidity. This confirmed the previous conclusion that Rhodamine 6G was not a suitable molecular probe for investigating the extent of water vapor permeation in both hydrophobic and hydrophilic aerogels.

This being said, there have been no humidity tests conducted on Rhodamine 6G aerogels dried using the Tristar degasser system. This is one area that will be investigated in the near future. It is quite possible that the Rhodamine 6G has a strong response to humidity and the aerogels containing this probe were simply not dried completely using the dessicator.

Fluorescein

From the fluorescence emission spectrum in Figure 16, it was clear that Fluorescein was both present and could be detected in silica aerogels. This meant the dye survived the fabrication and that the probe was successfully incorporated

into the aerogel. Fluorescein, then, was a viable option as an optical probe of silica-based aerogels fabricated via Union College's RSCE process.

From Figure 17, it can be seen that as humidity increased, the Fluorescein emission signal intensity decreased when the 5×10^{-4} M 100 % TMOS Fluorescein aerogel was dried in a dessicator. This was in agreement with McGaughey et al., who reported that there was a change in the emission intensity of the Fluorescein molecular probe with a variation in the relative humidity.[16] The response of Fluorescein observed in this research was deemed to be insufficient for establishing a response of the signal to humidity as it was again less than 0.1% in each humidity test conducted. The insufficient percent changes in signal can be seen in Table 5.

The Fluorescein aerogels were then dried in a Tristar degassing system and humidity tests carried out the same way. As seen in Table 6, the calculated percent loss in signal due to increasing humidity was more substantial than any of the other tests conducted as a loss of at least 0.1% in signal was observed. This was promising as this was the biggest response observed in the project at that time. At the time, the positive responses of Fluorescein to humidity in Table 6 were chalked up to error. This was because they were contradictory to the previous decrease in signal intensity of Fluorescein in response to an increase in humidity. It was concluded that the project should move forward with Fluorescein as the molecular probe as it had the largest response to changing humidity.

Since the response was a decrease in signal as humidity increased and we were utilizing a luminescent dye, it was necessary to calculate how much of the decrease in signal was due to the photodegradation of the dye rather than a change in signal due to humidity. The goal was to isolate the response of the signal to variations in humidity from the response due to the photobleaching of the dye. The range of percent signal lost due to photobleaching varies quite a bit between different gels as well as with different tests of the same gel which can be seen in Table 7. This meant that it was hard to pinpoint the exact amount of signal that was lost due to photobleaching between samples or even in one sample. Furthermore, the photobleaching for sample N6 was found to be responsible for a -0.066% change in signal which makes up a large portion of the total percent of signal lost in the initial crude humidity tests with the Fluorescein probe. For example, the N6 percent responses to humidity were -0.131%, -0.102%, and -0.165%. It can be seen here that the percent of signal lost due to photobleaching makes up about half of the total calculated response of the probe to humidity. This can be seen again in the P16 samples as they had photobleaching values greater than -0.070% but had only a -0.045% response to the humidity test (Tables 7 and 6 respectively). This implies that the overall signal change due to humidity was much smaller than initially thought (less than 0.1% for N6) and may not even be present as some photobleaching responses were greater than the humidity test (for example, P16). Since the photobleaching comprised such a large portion of the overall signal, the change in signal of Fluorescein to an increase in humidity in this research was concluded to be insignificant.

Fluorescein Breakthrough

Eventually, it was noticed that the Tristar degasser system used to dry the aerogels was not properly flowing nitrogen gas into the tube containing the sample to be dried. The gas flow issue was corrected and humidity tests redone. As seen in Figure 18, there was a large increase in the signal emission intensity as the aerogel was allowed to equilibrate with the room humidity once dried in the Tristar degasser properly. Although this was opposite what was originally observed, it was thought to be a more accurate representation of the response of the dye-doped aerogel to humidity.

The percent changes of each humidity test, visible in Table 8, were much more significant than the previous percent changes observed. Previously they were 0.1% or less but they increased to 7.0% and greater, so we were certain that we were observing a change in response due to a change in humidity. Furthermore, it was observed that there was a substantial and significant change in the emission signal in each aerogel regardless of the degree of hydrophobicity. Even in the 50%TMOS/50% MTMS samples there was a 7.0% and 10.6% response in the O14 and O13 samples respectively. This is a key finding as it implies that water vapor was still able to permeate into these hydrophobic aerogels and trigger a response of the probe. This is a unique discovery that must be considered in the future in dealing with commercial applications of hydrophobic aerogels.

Furthermore, there was an indication of a possible trend of increasing response to humidity as the aerogel became less hydrophobic. This implied that

as the aerogel becomes more hydrophobic in nature, less water vapor permeates into the aerogel. However, the percent responses to signal are extremely close to each other with some of the percent responses overlapping. This was the case with the 75% TMOS P16 which had a measured response of 16.7%. This response exceeds all the responses for the 100% TMOS N samples in Table 8. It is therefore difficult to say for certain that there is a definitive trend present relating the degree of hydrophobicity to the extent of water vapor permeation through the aerogel. Further testing will be done in this area to obtain more statistically significant results in order to verify or refute the presence of a trend relating the degree of hydrophobicity of an aerogel to the extent of water vapor permeation.

Lastly, from the data shown in Figures 19, 20, and 21, it appears that the hydrophobic aerogels have a larger initial response to humidity and then a smaller response towards the end of the test whereas the hydrophilic aerogels have a more constant response. If it was true there was no discernible trend relating the degree of hydrophobicity to the extent of water vapor permeation in the aerogel, then this would imply that the water vapor is actually permeating the hydrophobic aerogels to the same extent and at a faster rate than the hydrophilic aerogels. It could be that the hydrophobic surface of the aerogel actually allows water vapor to pass over it much easier than the hydrophilic aerogels. Again, further testing in this area is needed to confirm these conclusions.

Humidity Apparatus

As seen in the fluorescence emission scan in Figure 22, there was no clear trend observed between the induced relative humidity of the apparatus and the emission signal intensity of the A16 100% TMOS 10^{-5} M Rhodamine 6G aerogel. It appeared that the flowing nitrogen gas had something to do with this observed change in emission intensity and that the change was not solely due to the variation in humidity. The nitrogen might have been shifting the location of the aerogel within the incident beam of light and therefore changing the fluorescence emission signal intensity.

From the emission spectrum in Figure 23, it is clear that altering the nitrogen flow, without changing the humidity, caused a significant change in the response. It is also clear that at lower flows of nitrogen, the emission intensity did not change significantly. It was concluded, then, that at higher flows of nitrogen, the low-density aerogel was being blown around by the flowing gas. This altered the position of the aerogel in the incident beam, which meant that emission was being collected from a different portion of the aerogel. We have not ascertained whether the probe is distributed evenly throughout the aerogel sample. At different areas within the aerogel, there could be a different concentration of probe, which could cause the observed variation in emission intensity. Moreover, the aerogel monoliths are not perfectly symmetric; therefore, emission could be sampled from a different volume of the aerogel, depending on its position in the cuvette. It was concluded then that the response seen in Figure 22 was not due to humidity. It was also concluded that the aerogel would have to be held in place

during these tests in order to ensure that the nitrogen gas would not move the sample and that any observed change in signal intensity was due to humidity and not local environment differences within the aerogel.

The solution to this issue turned out to be hot gluing the aerogel to the bottom of the cuvette. Subsequently, continuous flowing nitrogen had no significant effect on the resultant fluorescence emission intensity of the Fluorescein probe, as seen in Figure 24. The constant exposure to nitrogen without the presence of humidity ensured that the aerogel was only experiencing the flow of nitrogen. Since the emission spectra did not change intensities during the constant flow, it appears that the aerogel was remaining in a fixed position within the apparatus and that the incident beam of light was contacting the sample in the same environment in each scan.

This seemed to solve the position issue but when the nitrogen gas was turned off and the aerogel was allowed to equilibrate with room conditions, there was a decrease in the fluorescence emission intensity of the Fluorescein molecular probe (Figure 24). This was puzzling as the crude Tristar tests prior to these have afforded a significant increase in signal with exposure to an increase in humidity upon drying with nitrogen. In order to test these results and see if they were real, a time based scan was collected in which the relative humidity and nitrogen flow was altered over time (Figure 25).

The time based scan (Figure 25) shows that when the nitrogen gas by itself was turned off, the Fluorescein signal decreased in intensity. It also shows that when the humidity was introduced into the apparatus, the Fluorescein signal also

decreased. Under high humidity (~90%) the signal continued to decrease and eventually leveled off. This was confirmation that the decrease in Fluorescein signal upon the increase of relative humidity was real and present in the humidity apparatus. This affirmed that the humidity apparatus displayed opposite results to that of the crude tests which afforded an increase in signal with an increase in humidity. Thus far, there has been no successful explanation as to why the humidity apparatus afforded an opposite response to the crude Fluorescein humidity tests performed previously and further work is needed to deduce the reason for the observed contradictory results.

Sessile Water Droplet Contact Angles

There was a slight difference between the contact angles before and after the image formatting (see Tables 9 and 10). For sample O13, for example, the measured contact angles were around 149 degrees prior to formatting and around 155 degrees after formatting. However, the trends of contact angle increasing as hydrophobicity increased were the same in both the pre- and post-formatting analysis. The properly formatted images were the ones that were considered the true measured contact angles.

The results from the contact angle measurements of the hydrophobic aerogels without probe matched up well with the angle measurements of the hydrophobic aerogels with probe. This can also be seen from the results in Table 10. This indicates that the addition of the probe to the hydrophobic aerogels had no appreciable effect on the hydrophobic nature of the aerogel.

The contact angle measurements, found in Table 10, for the P13 and P14 (75% TMOS / 25% MTMS) doped aerogels were around 140 degrees. This is in agreement with the range of contact angles previously recorded in the lab by Emily Green[7] for aerogels of corresponding degrees of hydrophobicity. The contact angle measurements for the O13 (50% TMOS / 50% MTMS) doped aerogel were around 155 degrees, which is also in agreement with the angles measured by Green[11] on aerogels with the same degree of hydrophobicity. This confirmed that the aerogels we were testing were indeed hydrophobic in nature. It also confirmed that the different aerogels were really of varying degrees of hydrophobicity and were therefore suitable for studies of hydrophobic aerogels.

Future Work

In the future, it would be prudent to examine some other molecular probes that might respond to humidity as well as the ones chosen. It would also be a good idea to go back and look at some of the molecular probes that were chosen but may have been overlooked do to the drying issues. One such probe is Rhodamine 6G which was ruled out as a probe due to its weak negative response to humidity. This ruling was made before the Tristar degassing system was fixed so there is no way to tell if this gel was completely dry before the humidity test was conducted. This probe should therefore be reexamined to determine its response to humidity.

It would also be useful to continue performing the crude humidity tests to see if there is a trend relating the degree of hydrophobicity to the extent of water

vapor permeation into the gel. As of now, an insufficient number of tests have been conducted for statistically significant data. More tests should be conducted in the future.

In the future, it would also be pertinent for students in the group to consider employing alternative methods for detecting humidity other than fluorescence detection. One of the methods listed in the Introduction chapter of this report, or one of the many other methods not listed, could be used in the future to detect the humidity within the aerogel matrix environment.

The main future goal of this project is to get the humidity apparatus functioning properly. This will allow us to move away from the crude humidity tests into a more quantitative and controlled test. The apparent negative response of the Fluorescein probe to humidity when in the humidity apparatus, as compared to the positive response in the crude test, must be understood before the humidity apparatus can be fully utilized for quantitative analysis.

References

(1) Pierre, A.; Pajonk, G. *Chem. Rev.* **2002**, *102*, 4243-4265.

(2) http://aerogel.nmcnetlink.com/aerogel-applications.html Accessed 5/19/09.

(3) http://www.supsalv.org/pdf/US%20Navy%20Diving%20R%20D%20T%20and%20E%20Programs.pdf Accessed 2/20/09.

(4) http://eetdnews.lbl.gov/cbs_nl/nl8/Aerogel.html Accessed 5/19/09.

(5) http://www.virtualacquisitionshowcase.com/docs/2008/PhysicalSciences-Brief.pdf Accessed 5/19/09.

(6) Figure by Smitesh Bakrania.

(7) Gauthier B.M.; Anderson A.M.; Bakrania S.; Mahony M.K.; Bucinell R. Method And Device For Fabricating Aerogels And Aerogel Monoliths. U.S. Patent 7,384,988, June 10, 2008.

(8) Gauthier, B.; Bakrania, S.; Anderson, A.M.; Carroll, M.K. *J. Non-Crystalline Solids* **2004**, *350*, 238-243.

(9) Rao, A.; Pajonk, G. *J. Non-Crystalline Solids* **2001**, *285*, 202-209.

(10) Schwertfeger, F.; Walther G.; Schubert, U. *J. Non-Crystalline Solids* **1992**, *145*, 85- 89.

(11) Green, E.; Melville, J.; Bono, M.; Anderson, A.M.; Carroll, M.K. *Books of Abstracts*, 235th ACS National Meeting, New Orleans, LA, United States, April 6-10, 2008.

(12) Harris, D. *Quantitative Chemical Analysis*, 7th ed.; W.H. Freeman and Company: New York, 2007.

(13) http://www.shsu.edu/~chemistry/chemiluminescence/JABLONSKI.html Accessed 5/19/09.

(14) Plata, D.; Briones, Y.; Wolfe, R.; Carroll, M.K.; Bakrania, S.; Mandel, S.; Anderson, A.M. *J. Non-Crystalline Solids* **2004**, *350*, 326-335.

(15) Phillips, A.; Mandel, S.; Anderson, A.M.; Carroll, M.K. *Books of Abstracts*, 231st ACS National Meeting, Atlanta, GA, United States, March 26-30, 2006.

(16) McGaughey, O.; Ros-Lis, J.; Guckian, A.; McEvoy, A.; McDonagh, C.; MacCraith, B. *Analytica Chimica Acta* **2006**, *570*, 15-20.

(17) Choi, Martin M.F.; Tse, O. *Ananlytica Chimica Acta* **1999,** *378*, 127-134.

(18) Otsuki, S.; Adachi, K. *Sensors and Materials* **1993,** *4*(6), 305-12.

(19) Lax, E.; Grondin, J.; Carroll, K.; Anane, S.; Mandel, S.; Passarelli, M.; Anderson, A.; Carroll, M. *Books of Abstracts*, 229th ACS National Meeting, San Diego, CA, United States, March 13-17, 2005.

(20) Lax, E. BS Chemistry Thesis, Union College, 2005.

(21) Boltinghouse, F.; Abel, K. *Anal. Chem* **1989**, *61*, 1863-1866.

(22) Zhu, Z.; Mason, J.; Dieckmann, R.; Malliaras, G. *Applied Physics Letters* **2002**, *81*(24), 4643.

(23) Geng, W.; Qiang, W.; Lu, W.; Li, J. *Journal of Physical Chemistry B* **2006**, *110* (43), 22029-22034.

(24) Takahashi, C.; Kitano, H. *Sensors and Actuators, B: Chemical* **1996**, 522-527.

(25) Melville, J. BS Mechanical Engineering Thesis, Union College, 2007.